

ENHANCED PHOTOTHERMAL AND ANTIBACTERIAL PERFORMANCE OF SILVER-DOPED MAGNESIUM FERRITE NANOCOMPOSITES

PROJECT REPORT

Submitted by

SONA THANKAM SUNNY

Register No.: AM23PHY012

Under the guidance of

Dr.ANN ROSE ABRAHAM

Assistant Professor

Department of Physics

Sacred Heart College (Autonomous), Thevara

Kochi – 682013

&

Dr. FRINCY FRANCIS

Assistant Professor

Department of Physics

St. Teresa's College (Autonomous), Ernakulam

Kochi – 682011

Submitted to

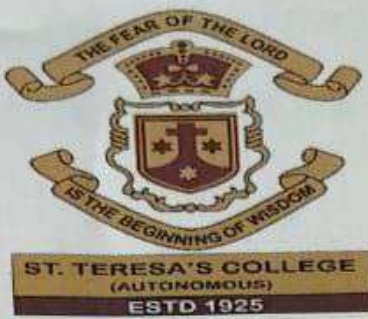
Mahatma Gandhi University, Kottayam

In partial fulfillment of the requirements for the award of the degree of
MASTER OF SCIENCE IN PHYSICS



DEPARTMENT OF PHYSICS

ST. TERESA'S COLLEGE (AUTONOMOUS), ERNAKULAM



CERTIFICATE

This is to certify that the project report entitled "**ENHANCED PHOTOTHERMAL AND ANTIBACTERIAL PERFORMANCE OF SILVER-DOPED MAGNESIUM FERRITE NANOCOMPOSITES**" is an authentic work done by **SONA THANKAM SUNNY (AM23PHY012)** under my guidance at Department of Physics, St. Teresa's College (Autonomous), Ernakulam for the partial fulfillment of the requirements for the award of the Degree of Master of Science in Physics during the year 2024-25. The work presented in this dissertation has not been submitted for any other degree in this or any other university.

Ann Rose

Supervising Guide

Dr. ANN ROSE ABRAHAM

Dr. FRINCY FRANCIS



Mary Vinaya
Head of the Department
DR. MARY VINAYA

Place: Ernakulam

Date: 3/05/2025

DEPARTMENT OF PHYSICS
ST. TERESA'S COLLEGE (AUTONOMOUS), ERNAKULAM



M.Sc. PHYSICS
PROJECT REPORT

Name : SONA THANKAM SUNNY
Register No. : AM23PHY012
Year of Work : 2024-2025

This is to certify that the project entitled "ENHANCED PHOTOTHERMAL AND ANTIBACTERIAL PERFORMANCE OF SILVER-DOPED MAGNESIUM FERRITE NANOCOMPOSITES" is an authentic work done by SONA THANKAM SUNNY.

Ann Rose

Staff member in-charge

Dr. ANN ROSE ABRAHAM

Dr. FRINCY FRANCIS

Assistant Professor



Mary Vinaya

Head of the Department

Dr. MARY VINAYA

Submitted for the university examination held at St. Teresa's College (Autonomous), Ernakulam.

Manoja
Dr. MANOJA

EXAMINERS :

DATE: 3/5/25

Dr. Louie Esther P.
Dr. LOUIE ESTHER P.

DECLARATION

I, SONA THANKAM SUNNY, a final year MSc. Physics student of the Department of Physics and Centre for Research, St. Teresa's College (Autonomous), Ernakulam, do hereby declare that the project report entitled "**ENHANCED PHOTOTHERMAL AND ANTIBACTERIAL PERFORMANCE OF SILVER-DOPED MAGNESIUM FERRITE NANOCOMPOSITES**" has been originally carried out under the guidance and supervision of **Dr.ANN ROSE ABRAHAM**, Assistant Professor, Department of Physics and Centre for Research, Sacred Heart College, Thevara and **Dr.FRINCY FRANCIS** Assistant Professors, Department of Physics, St. Teresa's College (Autonomous), Ernakulam in the partial fulfilment for the award of the Degree of Master of Physics. I further declare that this project is not partially or wholly submitted for any other purpose and the data included in this project is collected from various sources and is true to the best of my knowledge.

PLACE: ERNAKULAM

DATE: 3/05/25


SONA THANKAM SUNNY



ST.TERESA'S COLLEGE (AUTONOMOUS)
ERNAKULAM

Certificate of Plagiarism Check for Dissertation

Author Name

FATHIMA NIDA , SONA THANKAM SUNNY

Course of Study

M.Sc. Physics

Name of Guide

Dr. Ann Rose Abraham , Dr. Frincy Francis

Department

Department of Physics & Centre for Research

Acceptable Maximum Limit

20

Submitted By

library@teresas.ac.in

Paper Title

ENHANCED PHOTOTHERMAL AND
ANTIBACTERIAL PERFORMANCE OF SILVER-
DOPED MAGNESIUM FERRITE
NANOCOMPOSITES

Similarity

8% AI-16%

Paper ID

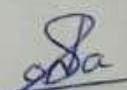
3556282

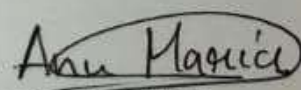
Total Pages

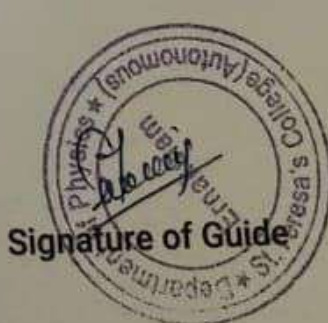
55

Submission Date

2025-04-29 09:59:35


Signature of Student


Checked By
College Librarian



Signature of Guide

ACKNOWLEDGEMENT

First and foremost, I would like to thank God Almighty for showering his blessings on me in this endeavour. I express my sincere gratitude to **Dr. ANN ROSE ABRAHAM**, Assistant Professor, Department of Physics and Centre for Research, Sacred Heart College, Thevara and **Dr. FRINCY FRANCIS**, Assistant Professors, Department of Physics and Centre for Research, St. Teresa's College (Autonomous), Ernakulam for her valuable guidance and constant supervision as well as for providing necessary information regarding the project.

I would also like to extend my gratitude to Ms. Vidhya Sivan, Research Scholar at the Department of Physics and Centre for Research, Sacred Heart College (Autonomous), Thevara, for being a constant support throughout this project.

I acknowledge my thanks to ms. Merin joby research scholar at the department of Physics and sender for Research Centre is a College Ernakulam for extending her support whenever sought.

I would like to express my sincere gratitude to the ASPIRE Scholarship program for providing financial support and encouragement throughout this project. The scholarship has enabled me to pursue my research interests and achieve academic excellence

I also express my gratitude to all the teaching and non-teaching staff members of the department for their valuable help and suggestions. I also extend my heartfelt gratitude to my parents and my friends who have willingly helped me out of their abilities to complete this project.

.

ENHANCED PHOTOTHERMAL AND
ANTIBACTERIAL PERFORMANCE OF
SILVER-DOPED MAGNESIUM FERRITE
NANOCOMPOSITES

ABSTRACT

This project explores the synthesis and characterization of magnesium ferrite (MgFe_2O_4) and silver-doped magnesium ferrite ($\text{Ag}-\text{MgFe}_2\text{O}_4$) nanocomposites, emphasizing their enhanced photothermal and antibacterial properties. The materials were synthesized via the sol-gel method and analyzed using X-ray diffraction (XRD), Field Emission Scanning Electron Microscopy (FESEM), UV-Visible spectroscopy and Fourier Transform Infrared Spectroscopy (FTIR). XRD analysis confirmed the spinel cubic structure and showed increased crystallite size upon silver doping. UV-Visible absorption and Tauc plots revealed tunable band gap energies, while FESEM images indicated improved particle distribution and morphology in doped samples. Photothermal analysis, conducted using a dual-beam thermal lens technique, showed that silver doping significantly enhanced thermal diffusivity. Antibacterial tests against *Escherichia coli* and *Staphylococcus aureus* confirmed superior antibacterial activity in silver-doped samples compared to undoped MgFe_2O_4 . The combined findings suggest that $\text{Ag}-\text{MgFe}_2\text{O}_4$ nanocomposite hold great promise for applications in biomedicine, environmental remediation, and photothermal therapy due to their multifunctional performance and improved efficiency.

CONTENTS

CHAPTER 1

1 INTRODUCTION.....	9
1.1 NANOTECHNOLOGY AND NANOSCIENCE	9
1.2 CLASSIFICATION OF NANOMATERIALS	9
1.3 PROPERTIES OF NANOMATERIALS	10
1.4 SYNTHESIS METHODS	10
1.5 ADVANTAGES OF NANOTECHNOLOGY	11
1.6 DISADVANTAGES OF NANOTECHNOLOGY	12
1.7 APPLICATIONS	12
1.8 MAGNETIC NANOPARTICLES	13
1.9 FERRITE	13
1.10 MAGNESIUM FERRITE NANOPARTICLE.....	15
1.11 SILVER DOPED MAGNESIUM FERRITE NANOPARTICLE.....	16
1.12 THE EFFECT OF SILVER DOPING ON THE PROPERTIES OF MAGNESIUM FERRITE NANOPARTICLES.....	16
1.13 REFERENCE.....	18

CHAPTER 2

2.1 SYNTHESIS METHODS.....	19
2.2 SOL GEL METHOD.....	19
2.3 SOL GEL METHOD FOR THE SYNTHESIS OF $MgFe_2O_4$ NANOPARTICLES..	20
2.4 SYNTHESIS $Ag-MgFe_2O_4$	21
2.5 CHARACTERIZATION.....	21
2.5.1 X-RAY DIFFRACTION.....	21
2.5.2 FIELD EMISSION SCANNING ELECTRON MICROSCOPY.....	23
2.5.3 FOURIER TRANSFORM INFRARED SPECTROSCOPY.....	24
2.5.4 UV-VISIBLE SPECTROSCOPY.....	24
2.6 APPLICATION.....	26

2.6.1 PHOTOTHERMAL TECHNIQUE.....	26
2.6.2 ANTIBACTERIAL ANALYSIS.....	32
2.7 REFERENCE.....	34

CHAPTER 3

3.1 X-RAY DIFFRACTION STUDIES.....	35
3.2 FIELD EMISSION SCANNING ELECTRON MICROSCOPY.....	38
3.3 UV- VISIBLE SPECTROSCOPY.....	39
3.4 FOURIER TRANSFORM INFRARED SPECTROSCOPY.....	41
3.5 PHOTOTHERMAL TECHNIQUES.....	42
3.6 ANTIBACTERIAL PROPERTY.....	44

CHAPTER 4

4.1 CONCLUSION.....	46
4.2 FUTURE SCOPE.....	48
4.3 REFERENCE.....	49

CHAPTER 1

INTRODUCTION

1.1 NANOTECHNOLOGY AND NANOSCIENCE

Nanotechnology is one of the promising technologies in this era. It is the branch of science which deals with the synthesis, usage and control of structures and devices by manipulating atoms and molecules at nanoscale in the range of 0.1 to 100nm. The term ‘nano’ derived from the Greek word ‘ bios’ means ‘dwarf’. Richard Feynman, an American physicist and Nobel prize winner introduced the concept of nanotechnology in his lecture “There’s plenty of room at the bottom” at Caltech in 1959. Later, Norio Taniguchi coined the term ‘nanotechnology’ in 1974. Nanotechnology encompasses the understanding of fundamental physics, chemistry, biology and technology of nanometer scale objects. Nanotechnology emerged as a revolutionary area with numerous applications in all fields of science. Nanoscience is the manipulation of molecules in the scale of nanometers and nanotechnology used in practical applications like devices. Nanoscience plays an important role in unveiling the potential of the nano world. Where quantum effects dominate, it is involved in understanding the fundamental principles that govern the behavior of materials at nanoscale, nanoscience is also an inter. This interdisciplinary science which means Almost all fields of science are getting involved. Due to quantum effects and ability to control surface area, nanomaterials show rare properties that are not exhibited by bulky materials. By utilizing these properties of nanomaterials, innovative materials and devices can be developed with the help of nanotechnology.

1.2 CLASSIFICATION OF NANOMATERIALS

When the size or dimension of a material is reduced into a nano range that's below 100 nm, dramatic changes in properties can occur. The type of nanomaterials can be determined according to the dimension they retain. Most properties of the nanomaterials that are helpful for the operation of immersion and prolixity are dependent on this dimension parameter. Therefore rested on confines, nanomaterials are classified into four. Zero-dimensional Nanomaterials with all three confines are in the nanoscale range. The performing structure is apprehended as an amount of fleck. It includes structures similar to nanospheres and nanoclusters. One-dimensional. If one dimension of material is reduced to the nano range while the other two dimensions remain large, a structure known as a quantum well is attained. This leads to needle-shaped nano paraphernalia. It includes structures similar as nano nanotube and nano rod. Two-dimensional, also the two confines of the material are reduced to the nano range , and the one dimension remains large. The performing structure is represented as a quantum wire. It includes nano film, nano layers, and nano coating within the nanometer range. This substantially exhibits a plate-like shape. Three-dimensional Nanomaterials having three arbitrary confines beyond the nano range,

that's over 100 nm. They aren't confined to the nanoscale range in any dimension. Bulk powders are an illustration of 3-D nanomaterials.

1.3 PROPERTIES OF NANOMATERIAL

The properties of nanomaterials include mechanical, electrical, thermal, and catalytic properties. Mechanical properties are the mechanical characteristics of accoutrements under different surroundings and colorful external loads. Different accoutrements have different mechanical properties. These mechanical properties of nanomaterials are due to a large number of surface atoms and interfaces, which leads to an increase in the viscosity of blights. Mechanical properties of nanomaterials include increased strength, rigidity, durability, hardness, and decreased pliancy. The electrical properties of nanomaterials depend on the confines, like the periphery and area of cross-section. Nanomaterials have high viscosity of grain boundaries, which reduces their conductivity. Due to the high density of defects, nanomaterials have high thermal expansion coefficients. The use of nanofluids will enhance the thermal transport. Mechanical properties are the mechanical characteristics of accoutrements under different surroundings and colorful external loads. Different accoutrements have different mechanical properties. These mechanical properties of nanomaterials are due to a large number of surface atoms and interfaces, which leads to an increase in the viscosity of blights. Mechanical properties of nanomaterials include increased strength, rigidity, durability, hardness, and decreased pliancy. The electrical properties of nanomaterials depend on the confines, like the periphery and area of cross-section. Nanomaterials have high viscosity of grain boundaries, which reduces their conductivity. Due to the high density of defects, nanomaterials have high thermal expansion coefficients. The use of nanofluids will enhance the thermal transport. Nanomaterials have distinctive optical characteristics such as increased scattering, absorption, and fluorescence. By changing the optic parcels, the size and shape of nanoparticles can be altered. Operations grounded on optic parcels include optic sensor, detectors, spotlights, photocatalysis, etc. Surface area affects catalytic activity. Since nanomaterials have a large number of facets, which will increase the surface area, leading to an increase in catalytic activity.

1.4 SYNTHESIS METHODS

Nanomaterials are synthesized by two different approaches, namely top-down and bottom-up. In the top-down approach, essence nanoparticles are synthesized by the corrosion of bulk essence using mechanical force or vaporization. In the bottom-up approach, it starts from the reduction of essence ions to essence snippets, followed by aggregation, resulting in the product of a nanoparticle.

Top-down styles

A top-down system is known as a destructive system. Lithography, ray ablation, sputtering, etc., are top-down styles. The main problem of this system is the fault of the face structure.

- In ball milling or mechanical grinding, the size reduction is achieved through the impact caused by the ball dropping from the top of the chamber where the source is placed.

- Nanolithography can produce a cluster with the desired shape and size.

In sputtering, the titles are ejected from the face of the material and it collides with energetic particles.

- In ray ablation, the nanoparticles are synthesized by striking an important ray on the target.

Bottom-up styles

The bottom-up approach is also known as a formative system. CVD, sol- gel, pyrolysis, etc. are bottom- up approaches.

- In the sol-gel system, condensation and hydrolysis are involved in the formation of nanoparticles. The advantage of this system should be the high stability of the nanoparticle and the achievement of an invariant nanostructure.

- In Chemical Vapor Deposition(CVD), a thin film of gaseous reactant is deposited on a substrate. By hitting the substrate, a chemical response occurs and this leads to the deposition of a thin film which can be recovered and reused.

- Hydrothermal and solvothermal styles are used in the production of nanowires, nanorods, and nanosheets.

- Pyrolysis is used in the large-scale production of nanomaterials. It's simple and cost-effective.

1.5 ADVANTAGES OF NANOTECHNOLOGY

Through nanotechnology, the natural properties of accoutrements can be changed, which leads to numerous operations. Some advantages of nanotechnology include;

- Nanotechnology enables new ways to gain and store energy. It helps in replacing fossil energies with renewable energy by making renewable energy sources like solar cells more effective and cheaper.

- By the use of nanochips, it's possible to erect veritably precise circuits at an infinitesimal position.

- It helps in the reduction of pollution. Nano pollutants are used in removing a wide range of adulterants.

- It helps in reducing the toxicity of medicines.

- In the medical field, nanotechnology is a boon. Nanoparticles are used in medicine delivery due to their small size and large surface area.

- The accoutrements which are created from nanotechnology are more precise, lighter, stronger.

1.6 DISADVANTAGES OF NANOTECHNOLOGY

Nanotechnology has many demerits too. Some of these include the following:

- Nanoparticles cause damage to human health as well as to the environment. For e.g., carbon nanoparticles cause infection in the lungs and have an adverse effect on the environment.
- Nanotechnology has the capability of producing dangerous weapons and drugs on a large scale. Atomic weapons are very destructive.
- By increasing the development in the field of nanotechnology, there is a high possibility of losing jobs in the farming and manufacturing industries.
- Nanotechnology is very expensive, and it is difficult to manufacture the nanoparticles since it is required to maintain certain conditions for their preparation.

1.7 APPLICATIONS

Nanotechnology is a promising field in this period. Presently, nanotechnology has achieved vast significance in nearly all fields from medicine to robotics. Nanotechnology has opened up possibilities in multitudinous operations and it increased the use of paraphernalia in nanometer scale. The operation of nanotechnology spans different sectors from medicine to energy and material wisdom. Nanotechnology, with its capability to manipulate matter at nanometer scale has revolutionized multitudinous industriousness and enabled the development of innovative operations with profound impacts. This field holds the pledge of shaping a future where paraphernalia are finagled at nanoscale, opening new borders in wisdom and technology. multitudinous operations in this field replaces or produce evolutionary development on being technologies. Some of the operations of nanotechnologies are mentioned below;

- **Energy resources:** Nanotechnology is used in the conversion and storage of energy, and it will enhance renewable energy sources. By making products of power from low-grade raw materials, which are cheaper, nanotechnology can address the deficiency of energy cells by adding mileage to machines and making products of power from normal raw materials. Nanostructured paraphernalia like quantum blotches and nanowires are used in designing solar cells, thus helping in reducing the cost of analogous renewable energy sources. Nanotechnology helps in increasing the effectiveness of solar cells.
- **Batteries:** Nano-finned paraphernalia can improve the charging time of batteries, and this will help in extending the battery life. Nano paraphernalia has a high face-to-volume ratio, so it will increase the battery capacity and power density. Nanotechnology plays a vital part in miniaturizing batteries for use in small-scale batteries.

- **Sensors:** Nano paraphernalia are used to make miniaturized sensors. This will enable the development of portable sensors that can indeed be used in biomedical operations. The large face-to-volume rate enables an increased commerce between the sensing element and the target analyte.
- **Water treatment:** Nanoparticles are used to purify artificial water pollutants in groundwater through chemical responses that are innocuous and at a lower cost.
- **Food sedulity:** Operations of nanotechnology in food security include manufacturing, packaging, and safety measures. Due to their high capability to repel absorption of moisture, light, and oxygen, nanomaterials are used in packaging.
- **Catalysis:** Nanomaterials are a good class of catalysts. Nanoparticles, which are used as catalysts, can achieve perfect selectivity and desirable activity.

1.8 MAGNETIC NANOPARTICLES

Magnetic nanoparticles are patches with sizes ranging from 1 to 100 nanometers, and they retain unique magnetic properties that differ from bulk accoutrements. These parcels are primarily due to the increased surface area and the amount of goods that crop at the nanoscale. Generally composed of accoutrements such as iron oxide, cobalt, or nickel, glamorous nanoparticles parade a miracle known as superparamagnetism. This means that the patches can be bewitched in the presence of an external glamorous field, but they lose their magnetization once the field is removed. The capability to control their glamorous parcels using an external field makes them protean for a wide range of operations. In the field of biomedicine, glamorous nanoparticles are used for targeted medicine delivery, where medicines can be carried precisely to specific spots in the body, reducing side effects and enhancing the effectiveness of treatments. They're also employed as discrepancy agents in glamorous resonance imaging(MRI) to ameliorate image quality. Also, glamorous nanoparticles have shown implicit in cancer treatment, particularly in hyperthermia therapy, where they're heated by an external glamorous field to destroy cancer cells. Beyond medical operations, these nanoparticles are also used in environmental remediation processes to remove adulterants, in data storage for high-viscosity information storage, and as catalysts in colorful chemical reactions due to their large surface area and reactivity. Despite their numerous promising uses, their safety, toxicity, and environmental impact remain important areas of ongoing exploration.

1.9 FERRITE

Ferrites are magnetic materials that combine electrical Ferrites are glamorous accoutrements that combine electrical and glamorous parcels, primarily conforming to iron oxide and essence oxide. They're liquid minerals formed by combining iron oxide with other essences. Spinel ferrites have

a structure of AB_2O_4 , where A and B represent tetrahedral and octahedral spots, independently. Metal spinel ferrite nanoparticles have the general molecular formula $MgFe_2O_4$ and a face-centered cubic close-packed structure. Among spinel ferrites, magnesium ferrite has been considerably studied. Its oxygen tiles borrow a boxy demitasse structure, and metallic cations occupy metal interstices in a unique two- lattice arrangement. The magnetization of spinel ferrites arises from the difference in glamorous moments of cations at octahedral and tetrahedral chassis spots. The resemblant arrangement of glamorous spins between the two sublattices leads to an endless glamorous moment. Spinel ferrites are extensively used in operations similar to glamorous recording, ferrofluids, glamorous resonance imaging, and more.

Magnesium ferrite, in particular, is used in many fields, including

- Magnetic operations
- Catalysis
- Biomedical operations
- Energy storehouse
- Detectors
- Water treatment

Its high glamorous performance, excellent chemical stability, low coercivity, and moderate achromatism magnetization make it suitable for soft glamorous operations at high frequency.

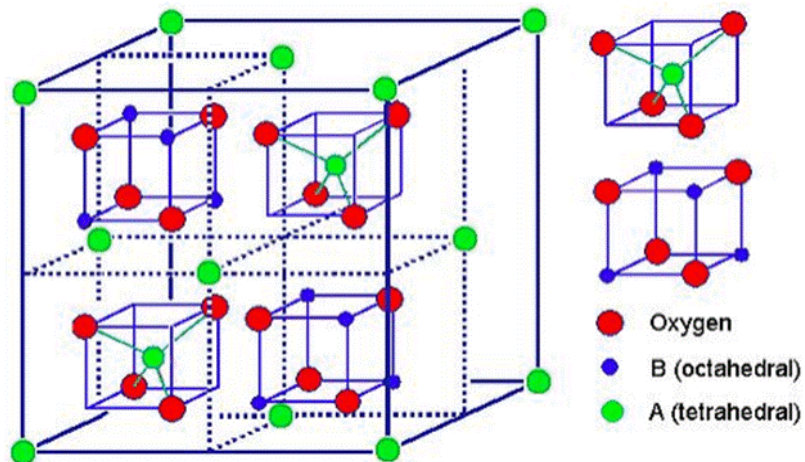


Figure 1.1: AB_2O_4 spinel structure¹

¹ <https://images.app.goo.gl/Ghamgq1HG1dYpDVa6>

1.10 MAGNESIUM FERRITE NANOPARTICLE

Magnesium ferrite (MgFe_2O_4) nanoparticles are spinel-structured nanomaterials known for their unique combination of magnetic and thermal properties, making them valuable across multiple scientific and industrial fields. Synthesized through methods like co-precipitation, sol-gel, or hydrothermal techniques, these nanoparticles typically range between 10 to 100 nm in size and exhibit ferromagnetic behaviour. Their structure allows for the substitution of magnesium ions into the iron oxide lattice, resulting in improved chemical stability and tunable magnetic properties. Due to their nanoscale size and high surface-area-to-volume ratio, MgFe_2O_4 nanoparticles can be engineered for enhanced performance in various physical and chemical environments. In biomedicine, magnesium ferrite nanoparticles have emerged as promising agents for targeted drug delivery, MRI contrast enhancement, cancer therapy, and especially photothermal and magnetic hyperthermia. In photothermal applications, these nanoparticles can absorb near-infrared (NIR) light and convert it into localized heat, effectively destroying cancer cells with minimal damage to surrounding healthy tissue. This capability, combined with their magnetic properties, enables dual-function therapies—where nanoparticles are guided to tumor sites with an external magnetic field and subsequently heated using NIR radiation or alternating magnetic fields. Their excellent biocompatibility and ability to be functionalized with targeting ligands or therapeutic molecules further enhance their effectiveness in clinical settings. Beyond medical uses, MgFe_2O_4 nanoparticles are gaining attention in environmental and energy-related applications, particularly in photocatalysis and water purification. Their magnetic properties make them easy to recover and reuse, which is essential for cost-effective and sustainable pollutant removal. Additionally, their surface can be modified with functional groups or combined with other materials to improve the adsorption of heavy metals, dyes, and other contaminants. In photothermal environmental applications, the heat generated under light exposure can accelerate catalytic reactions, improving the efficiency of pollutant degradation. This multifunctionality positions magnesium ferrite nanoparticles as a powerful tool in advancing both health care and environmental technologies. Major applications include;

- **Magnetic operations:** Magnetic resonance imaging, glamorous storehouse
- **Biomedical operations:** Targeted remedy, medicine delivery, biosensing
- **Catalysis:** Chemical responses, pollution remediation
- **Energy storehouse:** Supercapacitors, batteries
- **Sensors:** Magnetic sensing, biosensing
- **Water treatment:** contaminant junking, water sanctification
- **Photothermal operations:** Cancer remedy, excrescence ablation, photothermal therapy

1.11 SILVER-DOPED MAGNESIUM FERRITE NANOPARTICLE

Silver doping is a widely used technique to enhance the properties of nanoparticles, including magnesium ferrite (MgFe_2O_4). By introducing silver ions into the MgFe_2O_4 lattice, the material's structural, optical, and magnetic properties can be tailored for specific applications. Silver doping has been shown to improve the photocatalytic, antibacterial, and photothermal properties of MgFe_2O_4 nanoparticles, making them suitable for a range of applications, including biomedical, environmental, and energy-related fields. The incorporation of silver ions into MgFe_2O_4 nanoparticles can lead to significant changes in their material properties. For example, silver doping can enhance the optical absorption of MgFe_2O_4 nanoparticles, leading to improved photothermal properties. Additionally, the antibacterial activity of MgFe_2O_4 nanoparticles can be significantly enhanced by silver doping, making them effective against a range of bacteria. The magnetic properties of MgFe_2O_4 nanoparticles can also be modified by silver doping, allowing for tailored magnetic behaviour. The effects of silver doping on MgFe_2O_4 nanoparticles depend on various factors, including the concentration of silver ions, the synthesis method, and the particle size. By optimizing these parameters, researchers can create silver-doped MgFe_2O_4 nanoparticles with tailored properties for specific applications. The development of silver-doped MgFe_2O_4 nanoparticles has opened up new avenues for research in fields such as biomedicine, environmental remediation, and energy storage, and holds promise for the creation of advanced materials with enhanced performance.

1.12 THE EFFECT OF SILVER DOPING ON THE PROPERTIES OF MAGNESIUM FERRITE NANOPARTICLES

Silver doping has a great impact on the properties of magnesium ferrite nanoparticles, such that they find applications in diverse fields.

Antibacterial Properties: Silver doping can dramatically improve the antibacterial properties of magnesium ferrite nanoparticles to render them effective against various bacteria. Antibacterial refers to a substance or material's capability to inhibit or destroy bacteria. This property plays an important role in infection prevention as well as public health. Antibacterial agents may attack bacteria by destroying their cell membranes, blocking their metabolic process, or inducing the release of reactive oxygen species that cause damage to bacterial cells. By preventing bacterial proliferation and growth, antibacterial agents can prevent infection spread and limit the development of antibiotic resistance. Efficient antibacterial agents are required in numerous applications, such as healthcare, water treatment, and food preservation, to ensure human health and wellbeing. The use of antibacterial agents has grown in significance because of the increase in antibiotic-resistant bacteria. Scientists are constantly looking for new and creative methods to

fight bacterial infections, such as using nanoparticles, antimicrobial peptides, and other novel agents. These developments have the potential to change the landscape of antibacterial research and offer new options for prevention and treatment of bacterial infections. Further, learning about the antibacterial mechanisms of action can help guide the design of more potent treatments and prevention strategies. Interestingly, silver doping has been found to enhance the antibacterial activity of magnesium ferrite, which increases its inhibitory action against bacterial growth and infection.

Photothermal Properties: Silver doping may enhance the photothermal property of magnesium ferrite nanoparticles toward efficient heat generation upon light irradiation. Photothermal therapy is a type of treatment in which light is used to create heat in a targeted area or material. Light is absorbed by a photothermal agent, where it is transformed into heat, which can then be utilized to destroy cancer cells, bacteria, or other target cells. The method has come into focus with its potential to deliver minimally invasive treatments that are highly spatially precise. Photothermal agents, including dyes or nanoparticles, are commonly used to increase light absorption and produce heat. These agents may be engineered to specifically target certain cells or tissues, enabling selective treatment. The heat produced by photothermal therapy can destroy targeted cells, resulting in cell death. The benefits of photothermal therapy are lower side effects, minimal harm to surrounding healthy tissue, and the possibility of treating cancer or antibiotic-resistant infections. The method is being investigated for a number of applications, such as cancer treatment, infection control, and tissue ablation. Through the use of light and heat, photothermal therapy presents a promising means of targeted treatments with enhanced results. Its potential for accuracy and effectiveness makes it a promising field of study. Interestingly, doping magnesium ferrite with silver can enhance its photothermal effect, which could improve its therapeutic effectiveness and broaden its applications in cancer therapy and infection prevention. The enhanced properties of silver-doped magnesium ferrite nanoparticles make them promising materials for various applications, including biomedical, environmental, and energy-related areas.

1.13 REFERENCE

1. Srinivas, Pothur R., et al. "Nanotechnology research: applications in nutritional sciences." *The journal of nutrition* 140.1 (2010): 119-124.
2. Kung, Harold H., and Mayfair C. Kung. "Nanotechnology: applications and potentials for heterogeneous catalysis." *Catalysis today* 97.4 (2004): 219-224.
3. Nasrollahzadeh, Mahmoud, et al. "An introduction to nanotechnology." *Interface science and technology*. Vol. 28. Elsevier, 2019. 1-27.
4. Lue, Juh Tzeng. "Physical properties of nanomaterials." *Encyclopedia of nanoscience and nanotechnology* 10.1 (2007): 1-46.
5. Wu, Q., Miao, W. S., Zhang, Y. D., Gao, H. J., & Hui, D. (2020). Mechanical properties of nanomaterials: A review. *Nanotechnology Reviews*, 9(1), 259-273.
6. Asha, Anika Benozir, and Ravin Narain. "Nanomaterials properties." *Polymer science and nanotechnology*. Elsevier, 2020. 343-359.
7. Valenzuela, Raul. "Novel applications of ferrites." *Physics Research International* 2012.1 (2012): 591839.
8. Franco, A., and M. S. Silva. "High temperature magnetic properties of magnesium ferrite nanoparticles." *Journal of Applied Physics* 109.7 (2011).
9. Ichiyanagi, Y., et al. "Magnetic properties of Mg-ferrite nanoparticles." *Journal of Magnetism and Magnetic Materials* 310.2 (2007): 2378-2380.
10. Abraham, Ann Rose, Sabu Thomas, and Nandakumar Kalarikkal. "An Overview of Prospects of Spinel Ferrites and Their Varied Applications." *Theoretical Models and Experimental Approaches in Physical Chemistry* (2018): 117.

CHAPTER 2

MATERIAL SYNTHESIS AND CHARACTERISATION

2.1 SYNTHESIS METHODS

Nanoparticles can be synthesized in two methods: top-down and bottom-up. In the top-down method, nanoparticles are prepared by decomposition of bulk metal by any mechanical forces, whereas in the bottom-up method, preparation begins from the reduction of metal ions to metal atoms, followed by aggregation, leading to the formation of nanoparticles. The top-down method involves mechanical milling, electrospinning, lithography, sputtering, arc discharge technique, and laser ablation. In this research, the synthesis of nanoparticles was carried out using the bottom-up approach, i.e., the Sol-Gel process. It is a method that has been extensively used to synthesize nanostructured materials since it is easy, cheaper, and does not involve very high temperatures to synthesize highly homogeneous materials.

2.2 SOL-GEL METHOD

Sol-gel processing is an essential category of bottom-up nanofabrication techniques, which improves the nanostructure design from every atom in every molecule. This method has been a crucial factor in the recent past, based on its singularity, simplicity and capability to produce high-standard nanostructures with properties of desired specifications. Through the application of chemical reaction to assemble nanostructures, sol-gel processing offers a strong tool for generating a wide variety of nanomaterials such as nanowires, nanoparticles and thin films. The sol-gel process is primarily employed for the synthesis of metal oxide nanoparticles. The sol-gel process is also cost-effective and needs chemical solution deposition after calcination, arrangement of hydrolysis and condensation, gelation, ageing process, drying of materials by calcination and finally crystallization. There are some merits in addition to demerits for the sol-gel process. The significant benefits are sol-gel synthesis can be employed to synthesize materials of different shapes, dense powders and thin films and get pure, size controlled stable and monodispersed nanoparticles range 20-200 nm and it is also easier to have precise control over the doping level. But the sol-gel technique has certain limitations like this process is very substrate dependent and gel formation is a slow process, which gives sol a time consuming fabrication method compared to other processes. Sol-gel process has gained prominence for the preparation of inorganic materials, genuine hydrolysis and condensation of molecular precursors.

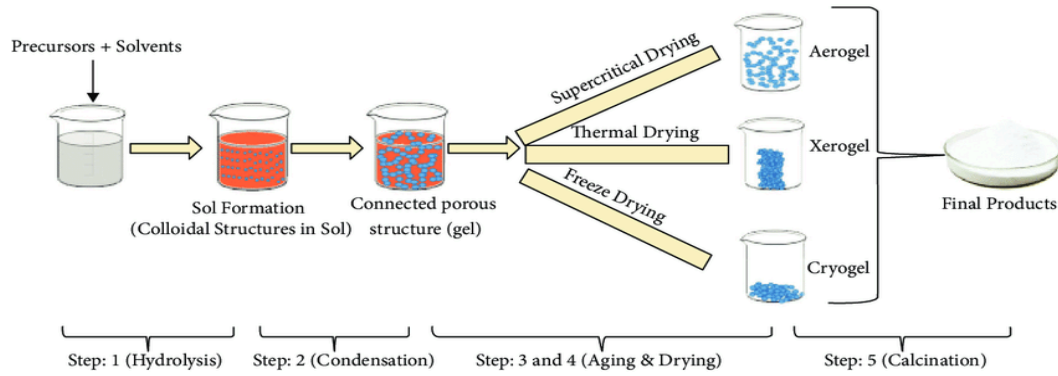


FIGURE 2.1: Schematic of different stages of sol-gel process²

2.3 SOL-GEL METHOD FOR THE SYNTHESIS OF MgFe_2O_4 NANOPARTICLES

In this study, sol-gel method was used to prepare MgFe_2O_4 nanoparticles by precursors like Magnesium nitrate ($\text{Mg}(\text{NO}_3)_2 \cdot 6\text{H}_2\text{O}$), ferric nitrate ($\text{Fe}(\text{NO}_3)_3 \cdot 9\text{H}_2\text{O}$), and polyvinyl alcohol (PVA) as precipitating agent.

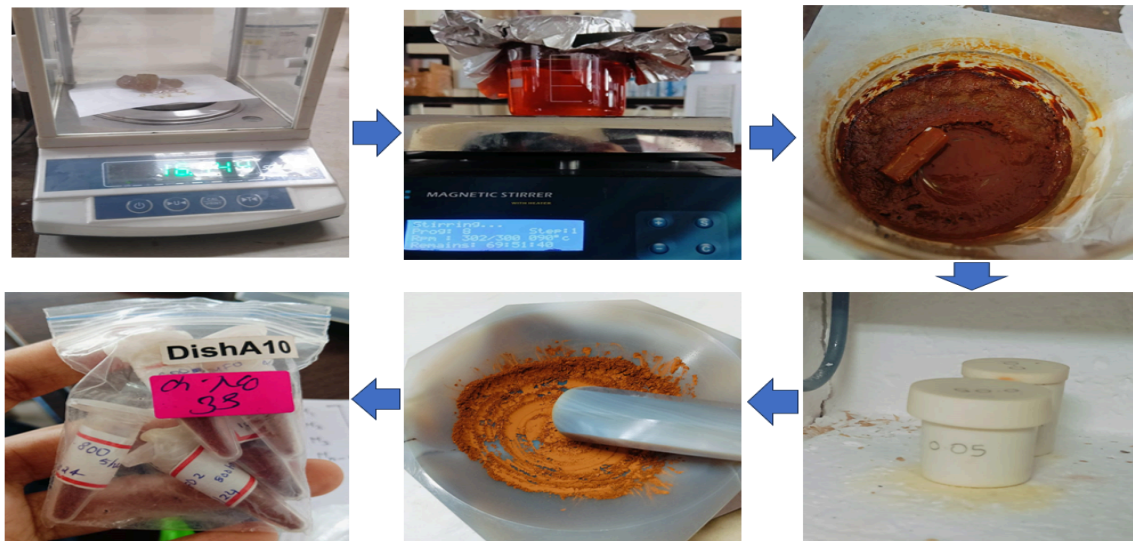


Figure 2.2: MgFe_2O_4

Aqueous solutions of $\text{Mg}(\text{NO}_3)_2 \cdot 6\text{H}_2\text{O}$ and $\text{Fe}(\text{NO}_3)_3 \cdot 9\text{H}_2\text{O}$ were prepared, blended, and sonicated. PVA was added to the mixture, and vigorous stirring was maintained until it was fully dissolved. The solution was evaporated at 60°C to give a viscous sol and subsequently a dark

² <https://images.app.goo.gl/uRAdnLDrHta8YJ1H8>

brown gel. The sample was dried and powdered, and then split and calcined at different temperatures (400°C, 600°C, 800°C) for 5 hours. The calcined samples were ground gently in an agate mortar using a pestle and filtered through a 100 µm mesh to give fine dark brown powders.

2.4 SYNTHESIS OF Ag-MgFe₂O₄

The synthesis of silver-doping magnesium ferrite nanocomposite is just same as that for magnesium ferrite nanoparticles, excepting that in this method the silver nitrate (AgNO₃) is added at a concentration of 0.05. The respective quantity of AgNO₃ used are just about 8.49 g, respectively. This doping procedure may affect the structural, magnetic, and optical properties of the obtained nanocomposites. The introduction of silver ions may enlarge crystallinity, alter particle size, and affect the overall performance of the material.

2.5 CHARACTERIZATION

2.5.1 X-RAY DIFFRACTION(XRD)

X-Ray diffraction (XRD) is a commonly used technique for analysing the crystallinity, phase composition, and structural characteristics of various materials. Using this method, X-ray beams are passed through it. Rather than utilizing considerably greater wavelengths, which would be unaffected by the spacing between atoms, x-rays beams are chosen due to their wavelength is similar to the spacing among atoms in the sample. This means that the angle of diffraction will be controlled by the distance of the atoms in the sample, the x-rays then go through the sample, “bouncing” off atoms in the structure to alter the trajectory of the beam at an angle different from the original beam, called theta. This is the diffraction angle. A number of these diffracted rays cancel one another out, but positive interference happens if the beams have matching wavelengths. When two x-ray beams with the same wavelength that are whole number integers combine, an additional beam with a higher amplitude is formed. This is known as constructive interference. For this particular angle of diffraction, the wave’s increased amplitude results in a stronger signal. The difference between the atomic planes can then be analysed from the angle of diffraction using Bragg’s law.

BRAGG’S LAW

Laue diffraction, which forms the angles of both coherent and incoherent scattering off a crystal lattice, is an exact example of Laue’s law known as Bragg’s law. An electronic cloud moves as an electromagnetic wave when x-rays strike a certain atom. Rayleigh scattering is the process by which the motion of these charges emits waves of a comparable frequency but somewhat blurred

due to several factors. The connection between an x-ray light beam and the reflection from a crystal surface is essentially explained by this law.

Bragg's law states that the x-rays angle of incidence, and angle of scattering are the same when it hits a crystal surface. Moreover, constructive interference will happen when the path difference d , is equal to wavelength, where n is a whole number.

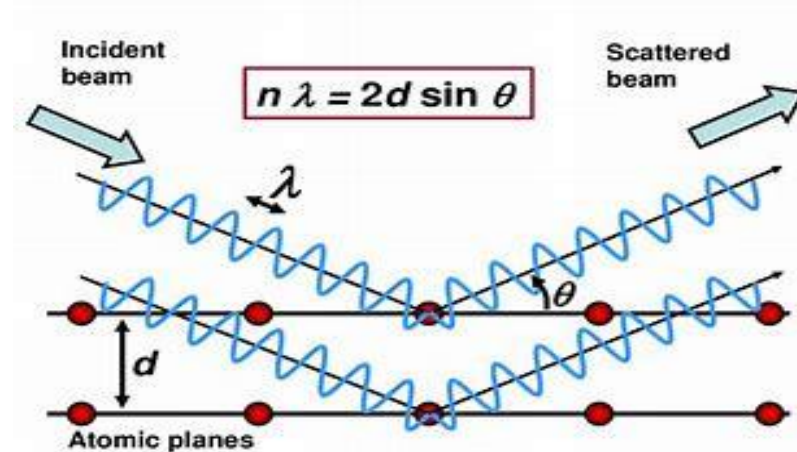


Figure 2.3: Principle of X-ray diffraction³

PARTICLE SIZE DETERMINATION FROM XRD

The result of X-ray diffraction exhibits the signal's strength for different diffraction angles at each of their corresponding two theta points. The following angle of diffraction coming from the incident x-ray beam transmitted into the sample determines the two theta positions, which corresponds to a specific spacing among atoms in the samples. The number of atoms within that phase with such spacing affects the peak's strength. The quantity of crystals or molecules with those particular spacing increases with peak intensity. There is an inverse relationship between Peak width and Crystal size. A larger crystal is connected with a thinner peak. The presence of a smaller crystal, a defect within the structure of the crystal, or an amorphous solid, which lacks ideal crystal structure, is expressed by a wider peak. The pattern recognised by XRD test can be used to identify a sample's composition for smaller samples. The patterns of diffraction for compounds, elements, and minerals are kept in a huge database of these substances. When the structure for a compound that is not known matches the position, width, and comparative altitudes of the diffraction patterns, the element's identity can be confirmed by evaluating it to values from the literature and experiments.

³ <https://images.app.goo.gl/D1neg3hbvkTCE59g7>

From the XRD spectrum the particle size of nano particle is calculated using the Debye Scherrer's formula

$$D = \frac{K\lambda}{\beta \cos\theta}$$

K=constant depend on crystalline shape

λ = X ray wavelength

β = FWHM

θ = diffraction angle

2.5.2 FIELD EMISSION SCANNING ELECTRON MICROSCOPY (FESEM)

Field emission scanning electron microscopy (FESEM) is a powerful imaging method founded on the concept of scanning a very narrow electron beam across a sample surface in order to create high-level images. The electron beam of Fe sum is created by a field emission gun (FEG), which shoots electrons under the influence of a strong electric field at extremely low voltages. This allows for the creation of A5 warrant electron beam with low energy speed, producing extremely high spatial resolution and negligible sample charging when the electron beam interacts with the surface atoms of the material that creates Secondary Electrons and backscattered electrons which are shown to create images that provide information on surface morphology, particle size and nanostructure features.

FESEM was utilized to study magnesium ferrite nanoparticles synthesized at different calcination temperatures. Effective imaging facilitated research into particle size and morphology evolution with changing temperature. At low synthesis temperature, the nanoparticles typically have smaller sizes and stronger agglomeration due to insufficient crystallization and high surface energy. At higher calcination temperature, FESEM images revealed an increase in particle size, enhanced Crystallinity and minimized agglomeration by providing fine visualization of nanoparticle surface texture and distribution. FESEM facilitated direct correlation between synthesis temperature and microstructural modifications.

2.5.3 FOURIER TRANSFORM INFRARED SPECTROSCOPY (FTIR)

FTIR is a analytical Technique Working For the identification of chemical bonds and functional groups within a material. It offers essential insights into the molecular structure, chemical composition and interaction mechanisms of a wide range of compounds. In FTIR spectroscopy, the absorption of infrared (IR) radiation by a material is analyzed, resulting in a distinctive spectral fingerprint decided by the materials molecular vibrations. This method is extremely Valuable in the research of nanomaterials and composite systems where it helps to clarify surface alterations, functionalization Process and interfacial bonding features.

Principle of FTIR

The basic principle of FTIR is based on molecular vibrational transitions. When a material is revealed to infrared radiations, particular wavelengths are absorbed, analogous to the natural vibrational frequencies of the chemical bonds within the molecules. These vibrational Involve stretching, bending, twisting, and rocking actions. Every type of bond and Functional group absorb IR radiation at characteristic frequencies permitting for their recognition and analysis. The absorption behavior Follows Beer's Lambert's law expressed mathematically.

$$A = \varepsilon/c$$

where ε is the molar absorptivity, a molecule-specific constant. The FTIR Instruments collect data in the time domains as an inner ferrogram, which files the intensity of the infrared signals as a function of the optical path difference. Transform algorithm is then utilized to convert the interferogram into a frequency domain spectrum, Usually plotted as absorbance or transmittance against wavelength, (cm^{-1})

An FTIR spectrometer often consists of an Infrared source that emits meat. Infrared radiations (4000 to 400 cm^{-1}). An interferometer produces an interference pattern through a beam splitter and mirrors ,a sample holder created for solids, liquid or gases and detectors. The following spectrum shows detailed information about molecular.Bonds, functional groups, and chemical interactions within the spectral library. Comparisons helping in precise material verification.

2.5.4 UV –VISIBLE SPECTROSCOPY

The range of electromagnetic waves that can be achieved by the objects in question is revealed by optical absorption. Absorption spectroscopy that functions within the ultraviolet- visible wavelength range is referred to as ultra-visible spectroscopy. This implies that it utilizes light within the visible and adjacent wavelength ranges. The visible spectrum absorption directly affects the observed color of the compounds involved. Molecules undergo electronic transitions within this part of the electromagnetic spectrum, and changes from the ground state to an excited state are what absorption discovers. This can also be used to assign additionally to find out the

band gap of the material. Part of incident radiation light that reaches a medium will pass through, while the rest of the wave will be absorbed. Electrons transition from a lower energy state to a higher energy state due to the absorption of photons. The absorption coefficient of a material is utilized in measuring its ability to absorb liquids and other substances.

It can be related through the expression whenever the material consists of a parabolic band structure

$$\alpha = K(h-Eg)^r/h$$

where 'Eg' is the band gap, α is absorption coefficient. The constant 'r' is a function of electronic transition nature. For direct allowed transition $r=1/2$, for indirect allowed transition $r=3$ and forbidden direct transition $1-3/2$. The absorption coefficient can be obtained from the absorption or emission spectra using the relation

$$I=I_0 \exp(-\alpha x)$$

Where 'I' is the transmitted intensity, ' I_0 ' is the intensity of the incident light and 't' is the thickness of the sample. The band gap energy can be determined by extrapolating the linear portion in the $h\nu$ versus $(\alpha h\nu)^2$. The absorption coefficient is a function of frequency

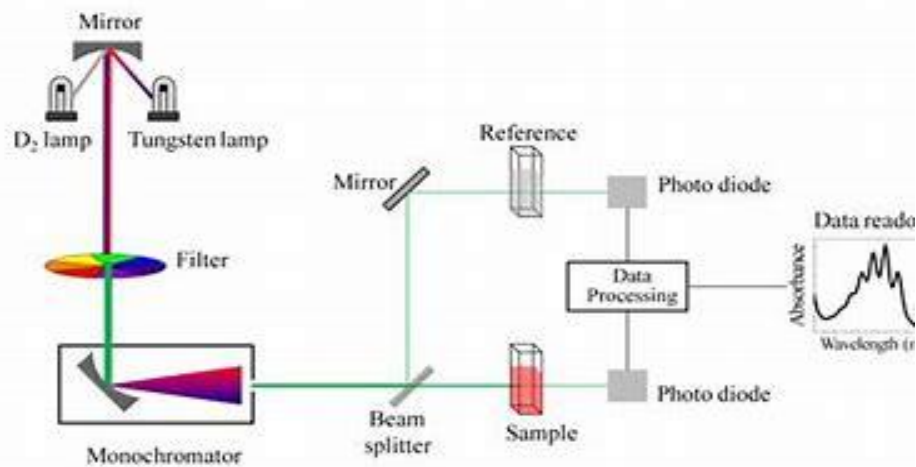


Figure 2.4: UV-vis-NIR spectrophotometer⁴

⁴ <https://images.app.goo.gl/gHYpkNfoSNoXC6kC8>

2.6 APPLICATIONS

PHOTOTHERMAL TECHNIQUES

The photothermal effect is a light-to-heat conversion process that is characterised by a temperature increase in a material due to the absorption of light. This process in nanomaterials has a variety of applications in multiple fields, ranging from renewable energy, biomedicine, wastewater purification, catalysis, etc. The photothermal performance of a nanomaterial is dependent on both its light-harvesting ability and its light-to-heat conversion efficiency. The photothermal effect occurs through mainly three major mechanisms: plasmonic localised heating, nonradiative relaxation of electron-hole pairs and thermal vibration of molecules. In the case of semiconductors like magnesium spinel ferrite, the major mechanism at play is non-radiative relaxation.

Photothermal Conversion via Non-Radiative Relaxation

When semiconductors are irradiated with electromagnetic radiation comparable to their band gaps, electron-hole pairs are generated. The energy of the excited electrons may be dissipated by the release of photons or through lattice vibrations, i.e., non-radiative transfer. The release of phonons instead of photons in a semiconductor through the recombination of charge carriers can increase heat loss and therefore lead to a local temperature increase of the lattice.

While the loss of energy in the form of heat is an undesirable effect in applications of semiconductors in electronics or as LEDs, the same effect can be used in applying semiconducting nanomaterials for water evaporation, targeted drug delivery, hyperthermia treatment, to act as sensors, etc.

Thermal Diffusivity

Thermal diffusivity is an intensive property of a nanofluid that is a measure of how fast it dissipates heat energy when subject to temperature changes. The role of thermal diffusivity in heat transfer is usually undermined as compared to thermal conductivity. The two properties are related, as thermal diffusivity may also be stated as the ratio of thermal conductivity to the product of density and specific heat capacity at constant pressure. The formula is:

$$\alpha = \frac{k}{\rho c_p}$$

k is the thermal conductivity, c_p is the specific heat capacity, ρ is density, ρc_p is the volumetric heat capacity

Thermal diffusivity is a measure of not just how quickly the material conducts heat but also of how much heat it can store. It indicates how the speed at which a material's temperature will adjust to a change in its thermal environment. While conductivity finds application in steady-state heat transfer, diffusivity becomes important in applications of transient heat transfer. Thus, the study of a nanofluid's thermal diffusivity is pertinent to its heat transfer application.

Experimental Techniques to Study Thermal Diffusivity

The **Laser Flash method**, developed by W.J. Parker in 1961, is a widely used technique for measuring thermal diffusivity. A short high high-intensity energy pulse from a laser or flash lamp causes thermal excitation of the sample. The energy absorbed is emitted back and causes a measurable temperature difference, which can be observed at its opposite rear face using an infrared detector. The temperature data thus obtained is fitted to the theoretical equations to obtain the value of thermal diffusivity. The underlying theory assumes that the thermophysical properties and density of the sample are constant within the temperature change induced by the flash (usually 2–10 °C). If all the above conditions are met, heat flow is one-dimensional and occurs throughout the thickness of the slab in the x direction. But in practice, the heat flow is not truly one-dimensional, and there are possibilities of radiative heat loss. Additionally, if the temperature rise is too large or too small, there could be significant deviations from the theoretical fit. However, with the right tuning of the experimental setup, the method can yield high-accuracy results.

Thermocouple-based methods may also be employed with the caveat of lower accuracy in exchange for a simple experimental setup that requires no sophisticated instrumentation for thermal excitation or measurement. In this method, the specimen is taken in a metal cylinder with a thermally conductive guard of the same material as the specimen. The cylinder's lower base is uniformly heated. Two thermocouples are used for temperature measurements. One is positioned laterally at the base to record the input temperature, while the other is positioned at the upper base to record the transient temperature. Readings are noted frequently every few seconds. The transient temperature from the upper thermocouple is compared to the ones obtained from the equations for the thermal field calculated using the measurement of the lower thermocouple. The method is best suited for highly conductive materials and requires a large amount of the sample.

Thermal Lens Spectroscopy (TLS) is a sensitive technique for measuring optical absorption and thermal properties by detecting refractive index changes induced by laser heating. When the sample is thermally excited by a laser beam, a temperature gradient is formed from the centre of the beam spot. The refractive index of the sample is temperature-dependent and thus is modified by the laser beam. This results in the formation of a thermal lens, first discovered by Gordon et al. in 1965. This lens causes beam divergence (as most substances expand on heating), which can

be observed as a signal of decreasing intensity. The formation of the lens is not instantaneous but takes place over a characteristic of the thermal properties of the sample.

TLS can be done with both single-beam and dual-beam laser setups. The single-beam thermal lens technique employs the same laser beam to both excite the sample and simultaneously probe the thermal lens signal. The setup is simpler as compared to a dual-beam configuration and contains fewer optical components, and avoids the alignment challenges of dual-beam systems. But it has lower signal-to-noise ratios and is limited to samples with minimal scattering.

Dual-beam setups involve a higher power laser to excite the sample (the pump laser) while a lower power laser beam serves as the probe. The pump is filtered out before the signal reaches the detector. The beams can be configured in either collinear or transverse fashion. The dual-beam setup is sensitive to traces of as low as parts per billion of solute in a solvent. Dual-beam thermal lensing can further be divided into mode-matched and mode-mismatched configurations. In the mode-matched configuration, both pump and probe beams have their focal points and waists coinciding at the sample. It produces the maximum thermal lens signal because the probe beam passes through the region of greatest refractive index change caused by the pump beam's heating. In the mode-mismatched configuration, the probe beam waist is typically larger and/or positioned at a different location than the excitation beam waist within the sample cell. The signal strength is generally lower than in the mode-matched configuration, as the probe does not sample the peak of the thermal lens effect.

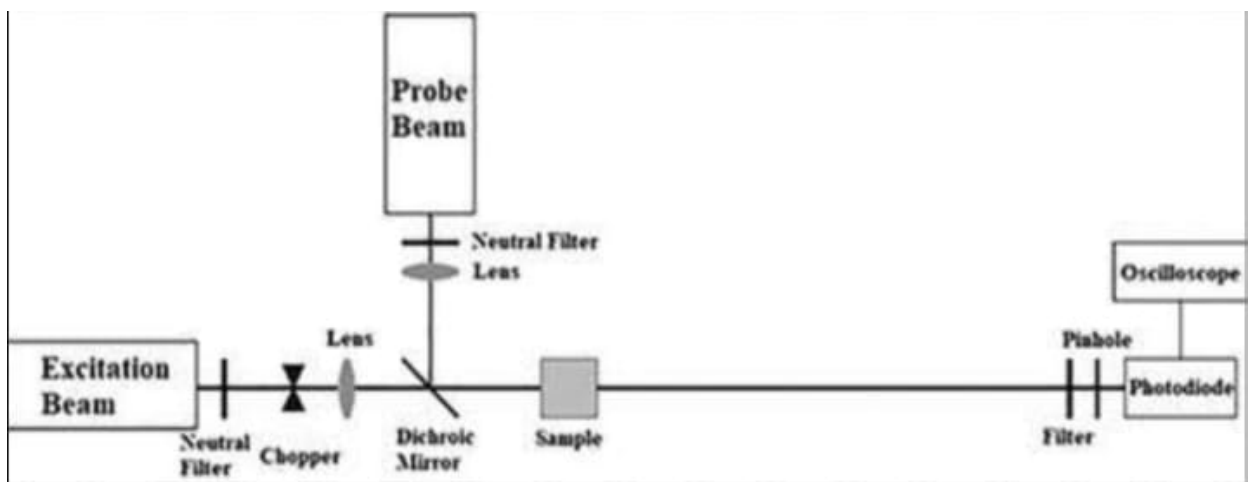


Fig: 2.5 Schematic diagram of dual-beam mode-matched TLS arrangement

Mode-Matched Dual-Beam Thermal Lens Technique

The thermal lens (TL) technique is highly sensitive and can detect extremely small changes in refractive index, down to about 10^{-8} across the laser beam's cross-section. These tiny changes result from very small temperature increases, as low as 10^{-5} °C, especially in liquid samples. The basic principle behind TL spectrometry is that a laser beam can heat a sample and cause changes in its refractive index. To observe this effect, a focused laser beam of a suitable wavelength is directed into the sample. This focusing creates an artificial beam waist, which depends on the laser's focal length (F), its initial beam size, and the laser wavelength (λ). As the sample absorbs energy, local heating occurs, increasing the temperature in that region. The temperature rise changes the refractive index of the medium, forming a thermal lens that can be converging or diverging. The direction of the lens depends on the temperature coefficient of refractive index (dn / dt) of the material. Most liquids form a negative thermal lens because they expand when heated, reducing their density and refractive index. To perform a TL experiment, we can either quickly open a shutter in front of the pump beam or deliver a single laser pulse, depending on whether we are using continuous wave (CW) or pulsed lasers. The lens takes time to form, and this duration depends on the rise time of the laser pulse and the thermal response time of the sample. During this lens formation, a second laser beam (probe beam) can be sent through the same region. As the sample heats, the probe beam spreads out, and this increase in beam size is known as thermal blooming. By observing how the probe beam changes, we can calculate dn/dt and other photo-thermal properties of the material. Instead of directly measuring the beam size, it's often easier to monitor how the intensity of the probe beam changes over time. In a mode-matched, collinear pump-probe setup, this becomes even more efficient. We can place a small aperture at the center of the undistorted probe beam. As soon as the pump laser is turned on, the thermal lens causes the probe beam to diverge, reducing the intensity detected through the aperture. A photo detector can easily record this drop in probe intensity, giving insight into thermal lens development.

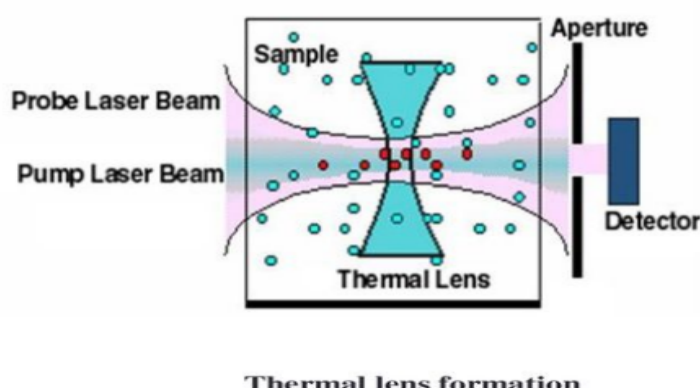


Fig 2.6 Thermal lens formation

Equation for Focal Length of the Thermal Lens:

When a continuous-wave (CW) laser beam starts interacting with a liquid at time $t=0$, the focal length F of the thermal lens can be calculated using:

$$\frac{1}{F} = \frac{P_{\text{abs}} \left(\frac{dn}{dt} \right)}{\pi k \omega^2 (1 + t_c/2t)}$$

where:

P_{abs} - Power absorbed by the liquid

K - heat conductivity of the liquid

w -beam radius

ρ -density

Also, $P_{\text{abs}} = P\alpha L$ for small αL

P -incident power

α -absorption coefficient

L -path length through the sample

The thermal lens starts with zero strength at $t = 0$ and gradually reaches a steady-state value. The formula is valid only for low-power levels, where spherical aberrations due to large phase shifts are avoided. To maintain accuracy, it's essential to set laser power, concentration, and optical path length to avoid visible aberration rings in the beam spot.

Time-Dependent Probe Intensity Equation:

When these conditions are met, the intensity of the probe beam changes over time according to:

$$I(t) = I_0 \left[1 - \theta \left(1 + \frac{t_c}{2t} \right)^{-1} + \frac{1}{2} \theta^2 \left(1 + \frac{t_c}{2t} \right)^{-2} \right]^{-1}$$

Expression for θ :

The value of θ relates to how much thermal power is absorbed and is given by:

$$\theta = P_{th} \left(\frac{dn}{dT} \right) \lambda_L k$$

Where:

dn/dT - temperature dependence of refractive index

λ - laser wavelength

k -thermal conductivity

The time constant t_c indicates how long the thermal lens takes to form. This value can be obtained by fitting the theoretical model to the experimental probe intensity data.

Thermal Diffusivity Equation

Once t_c is known, we can calculate the thermal diffusivity (D) using:

$$t_c = \frac{\omega^2}{4D}$$

Advantages of Mode-Matched Dual-Beam Thermal Lens Technique

In mode-matched systems, the pump and probe beams are the same size as the sample. This makes it easy to align the setup and simplifies the theory behind the experiment. It also helps reduce possible errors. Because the beams overlap well and have equal sizes, the measurements are stable and can be repeated reliably. This is helpful for regular testing and comparing different samples. The technique is very sensitive and works well even with clear or weakly absorbing samples. This method has been used successfully on gases, liquids, and solids. That makes it useful for studying many kinds of materials. The method does not damage the sample, and it only requires a small amount of material. This is especially useful when the sample is rare or limited.

Limitations of Mode-Matched Dual-Beam Thermal Lens Technique

Because the beam sizes are fixed to be equal, it is harder to adjust the setup to improve the signal-to-noise ratio. This makes it difficult to detect very low absorbance levels in some samples. The thermal lens in a mode-matched system can be more prone to optical distortions. If these aren't corrected in the theory or setup, they can reduce the accuracy of the results.

2.6.2 ANTIBACTERIAL ANALYSIS

Antibacterial testing analyzes the ability of compounds to inhibit or remove bacterial growth, which is a crucial element in the development of antimicrobial agents for application in healthcare, food preservation and Environmental Protection. During such testing, researchers attain essential insights into the efficacy and mechanisms of action of antibacterial materials, Thus informing the design and optimization of new anti microbial solutions. Various established methods are applied for antibacterial assessment Among the disc diffusion assay were zones of inhibition around a disk serve as a measure of antibacterial activity; The broth dilution essay, Which defines the minimum inhibitory concentration (MIC) essential to prevent bacterial growth; and the agar well diffusion assay, which evaluates bacterial susceptibility to test compounds based on the formation of inhibition zones around well containing the test substance.

Among these The well Agar diffusion assay, sometimes referred to as the shooting method, provides a especially effective technique for assessing the antibacterial activity of materials such as $MgFe_2O_4$ or $Ag-MgFe_2O_4$ offer nanoparticles against common bacterial strains like *Escherichia coli* and *staphylococcus aureus*. Distinct from the disk diffusion method, the well diffusion as essay involves the uniform inoculation of Muller hinton Agar plates with a standardized bacterial suspension typically adjusted to a 0.5 McFarland standard to ensure reproducibility. Small wells. Usually 5 - 8 mm in diameter, are then precisely created in the Agar using a sterile coat borer or micro pipette tip into which 20 - 100 μL of nanoparticles suspension is. With precision, securing no air bubbles or overflow occur. The plates are subsequently incubated at 37°C for 18 - 24 hours, after which clear zones of inhibition surrounding the wells suggest antibacterial activity; these zones are carefully measured to allow comparison of efficacy over different samples or concentrations.

This method, providing the advantage of accommodating larger sample volumes analyzed to disk diffusion, provides increased sensitivity, particularly for compounds with limited diffusion capability though it Necessitates strict control of well dimensions, sample volume, and bacterial inoculation consistency to verify reliable and reproducible results. Antibacterial materials evolved through such testing methods have extensive applications across multiple sectors: in healthcare, antimicrobial coatings on medical devices help avoid infections; in the food industry, antibacterial packaging materials extend shelf life by minimizing microbial contamination; an in environmental sectors, especially water treatments, antibacterial agents are critical for removing pathogenic microorganisms and providing safe drinking water. As antibiotic resistance continues to appear as a global threat the strict testing and analysis of new antibacterial agents remain more important than ever to force the development of effective, sustainable and innovative antimicrobial solutions.

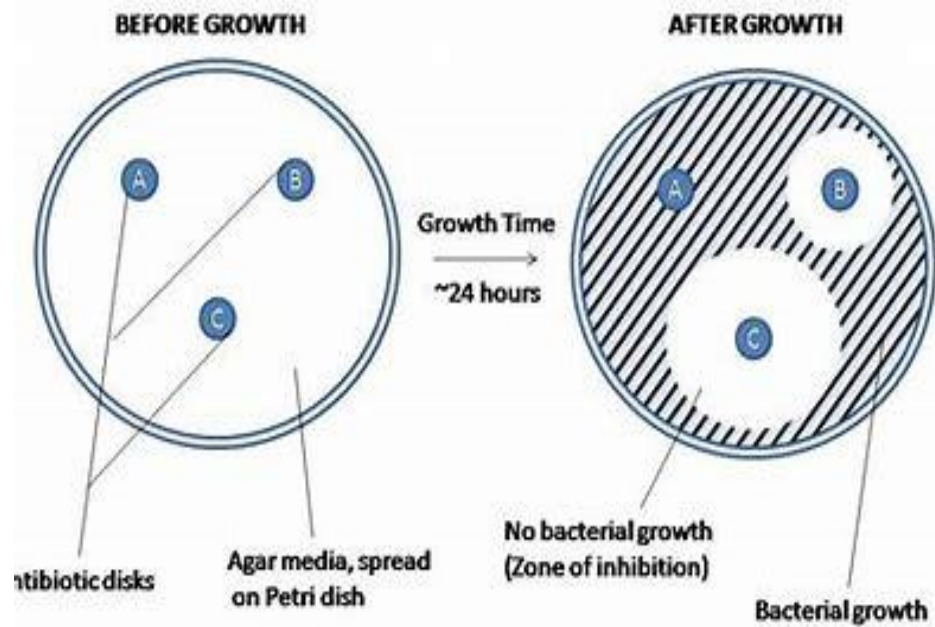


Fig 2.7: Well Diffusion Method

2.7 REFERENCE

1. Sundari, Rita, et al. "The characterization study of ferrites (magnesium and manganese) using sol gel method." *The Malaysian Journal of Analytical Sciences* 18.3 (2014): 485-490.
2. Bokov, D., Turki Jalil, A., Chupradit, S., Suksatan, W., Javed Ansari, M., Shewael, I. H., ... & Kianfar, E. (2021). Nanomaterial by sol-gel method: synthesis and application. *Advances in materials science and engineering*, 2021(1), 5102014.
3. Hench, Larry L., and Jon K. West. "The sol-gel process." *Chemical reviews* 90.1 (1990): 33-72.
4. Chihi, I., et al. "Sol-gel synthesis and characterization of magnesium ferrites by XRD, TEM, EPR, Mossbauer, and impedance spectroscopy." *Journal of Materials Science: Materials in Electronics* 32 (2021): 16634-16647.
5. Epp, J. "X-ray diffraction (XRD) techniques for materials characterization." *Materials characterization using nondestructive evaluation (NDE) methods*. Woodhead Publishing, 2016. 81-124.
6. Fatimah, S., Ragadhita, R., Al Husaeni, D. F., & Nandiyanto, A. B. D. (2022). How to calculate crystallite size from x-ray diffraction (XRD) using Scherrer method. *ASEAN Journal of Science and Engineering*, 2(1), 65-76.
7. Speakman, Scott A. "Estimating crystallite size using XRD." *MIT Center for Materials Science and Engineering* 2.14 (2014): 03-08.
8. Hajipour, Mohammad J., et al. "Antibacterial properties of nanoparticles." *Trends in biotechnology* 30.10 (2012): 499-511.
9. Baig, Nadeem, Irshad Kammakakam, and Wail Falath. "Nanomaterials: A review of synthesis methods, properties, recent progress, and challenges." *Materials advances* 2.6 (2021): 1821-1871.
10. Sharma, Anwesha, et al. "NANOMATERIALS AND NANOTECHNOLOGY: A COMPREHENSIVE STUDY OF SYNTHESIS, CHARACTERIZATION AND MULTIFACETED APPLICATIONS." *Biochemical & Cellular Archives* 23 (2023).
11. Titus, Deena, E. James Jebaseelan Samuel, and Selvaraj Mohana Roopan. "Nanoparticle characterization techniques." *Green synthesis, characterization and applications of nanoparticles*. Elsevier, 2019. 303-319.
12. Makuła, Patrycja, Michał Pacia, and Wojciech Macyk. "How to correctly determine the band gap energy of modified semiconductor photocatalysts based on UV-Vis spectra." *The journal of physical chemistry letters* 9.23 (2018): 6814-6817.

CHAPTER 3

RESULTS AND DISCUSSIONS

3.1 X-RAY DIFFRACTION STUDIES

a)XRD SPECTRUM OF MgFe₂O₄

In this work, structural characterization is done using X-ray diffraction method. The XRD results showed that the magnesium ferrite sample calcined at 800°C exhibited the highest purity and crystallinity compared to other temperatures. Therefore, the 800°C calcined sample was selected as the optimal material for further studies, and silver was doped into this sample to investigate its effects. The samples are denoted as MFO1, MFO2, and MFO3, corresponding to magnesium ferrite calcined at 400°C, 600°C, and 800°C, respectively.

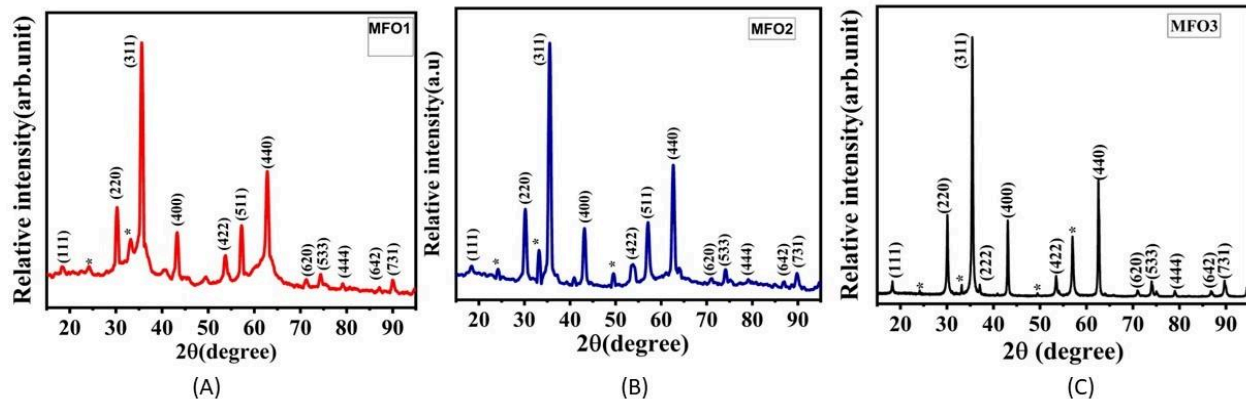


Fig 2.8 : XRD pattern of MgFe₂O₄ (A)-400°C ,(B)-600°C ,(C)-800°C

Fig 2.8 shows the XRD plot of MgFe₂O₄ which was plotted and analysed using origin software. On comparing the peaks with the provided JCPDS File, it is found that the prepared MgFe₂O₄ is in accordance with the data and is having a cubic structure.

The crystalline size of MgFe₂O₄ are investigated using Debye- Scherrer Formula as shown in b

$$D = \frac{K\lambda}{\beta \cos\theta}$$

$$D = 0.94 * 0.15406 / 0.32519^0 * \cos(17.7303)$$

$$D = 26.78 \text{ nm}$$

Here, K represents the shape factor, with a specific value of 0.9678. The symbol λ corresponds to the wavelength of Cu-K α radiation (1.54 Å), θ denotes Bragg's angle measured in degrees, and β signifies the Full Width at Half Maximum (FWHM) of the diffraction peak. This formula

serves as a means to estimate the average size of crystalline samples based on X-ray diffraction data, providing valuable insights into the structural characteristics of the material under investigation. The 2θ value of major peak, average crystallite size (D), FWHM values of the sample are analysed in table

The crystallite size was measured as 26.78 nm. This measurement indicates that the synthesized nanoparticles exhibit nanoscale crystallinity. The observed crystallite size, derived from X-ray diffraction (XRD) peak broadening, suggests that the synthesized nanoparticles are finely crystalline and uniform, consistent with effective control of particle growth during synthesis. The obtained peaks were compared with the JCPDS file. In addition, XRD data was utilized to calculate microstrain and dislocation density of this sample using the Williamson-Hall method.

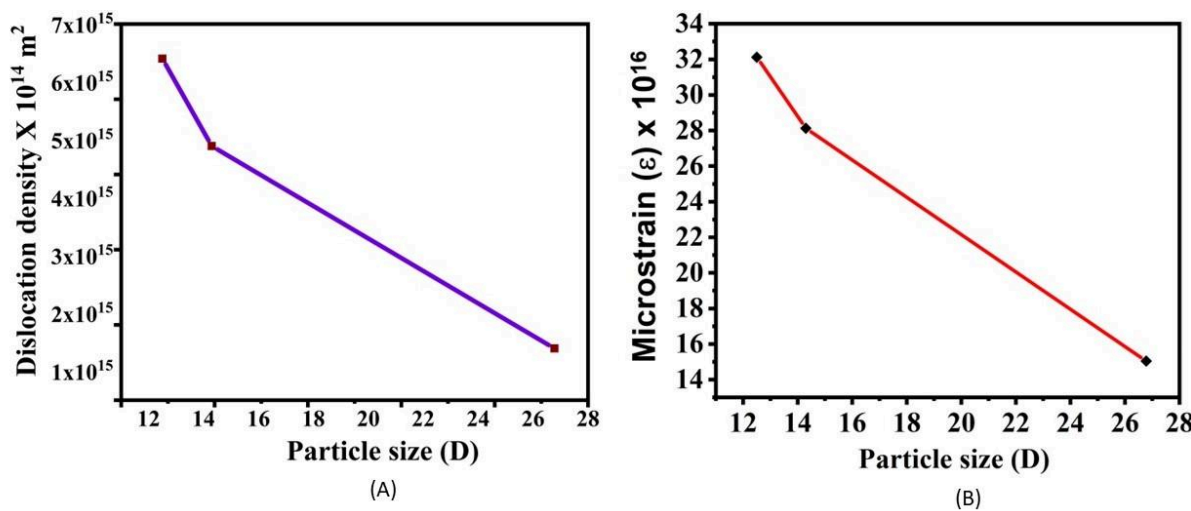


Fig 2.9: dislocation density (A) and Microstrain (B) graph

Sample Name	FWHM	Crystalline Size (nm)	Dislocation	Microstrain
MFO 1	0.69676	12.50	6.4	32.122
MFO 2	0.60932	14.30	4.8902	28.1335
MFO 3	0.32519	26.78	1.39437	15.0523

XRD Analysis Results

b) XRD SPECTRUM OF Ag- MgFe2

The XRD spectrum of silver-doped magnesium ferrite with a silver concentration of 0.05 is presented in Figure 3.1. The observed peaks are compared with the JCPDs file and it is found that the prepared sample is in accordance with the data and is having a cubic structure. The sample are denoted MAg05FO, representing magnesium ferrite ($MgFe_2O_4$) doped with silver (Ag) concentration of 0.05, respectively.

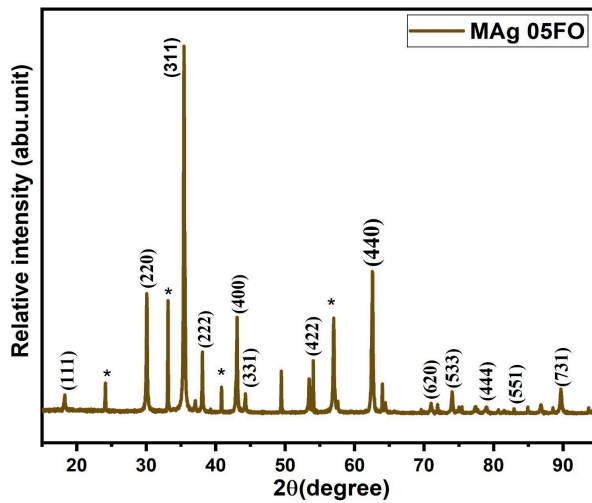


Fig 3.1: XRD spectrum of silver doped magnesium ferrite.

The crystalline size of $Ag_{0.05} - MgFe_2O_4$ are investigated using Debye- Scherrer Formula as shown in b

$$D = \frac{K\lambda}{\beta \cos \theta}$$

$$D = 0.94 * 0.15406 / 0.23317^0 * \cos(17.72496)$$

$$D = 33.89 \text{ nm}$$

XRD analysis result

Sample name	FWHM	Crystalline size
MAg05FO	0.23317	33.89 nm

The crystalline size of $Ag-MgFe_2O_4$ was found to be 33.89 nm for 0.05 concentrations.

The incorporation of silver into magnesium ferrite significantly influences its structural properties. Undoped magnesium ferrite exhibits crystallite sizes ranging from 12.50 to 26.78 nm. In contrast, silver-doped magnesium ferrite shows an increased crystallite size of 33.89 nm, accompanied by a decrease in FWHM values. This suggests that silver doping promotes grain growth and enhances crystallinity, potentially improving the material's properties.

3.2 FIELD EMISSION SCANNING ELECTRON MICROSCOPY (FESEM)

The surface morphologies of the synthesized samples are examined using FIELD EMISSION SCANNING ELECTRON MICROSCOPY (FESEM). This method is mainly used for the analysis of particle size and its distribution, surface morphology, and elemental composition.

The FESEM images of MgFe_2O_4 are represented in figure 3.2. The FESEM image of the magnesium ferrite sample reveals a spherical shape, indicating a uniform morphology. The particles appear to be agglomerated, forming clusters. The surface texture appears smooth, suggesting a well-defined structure. These morphological features can significantly influence the material's properties and potential applications.

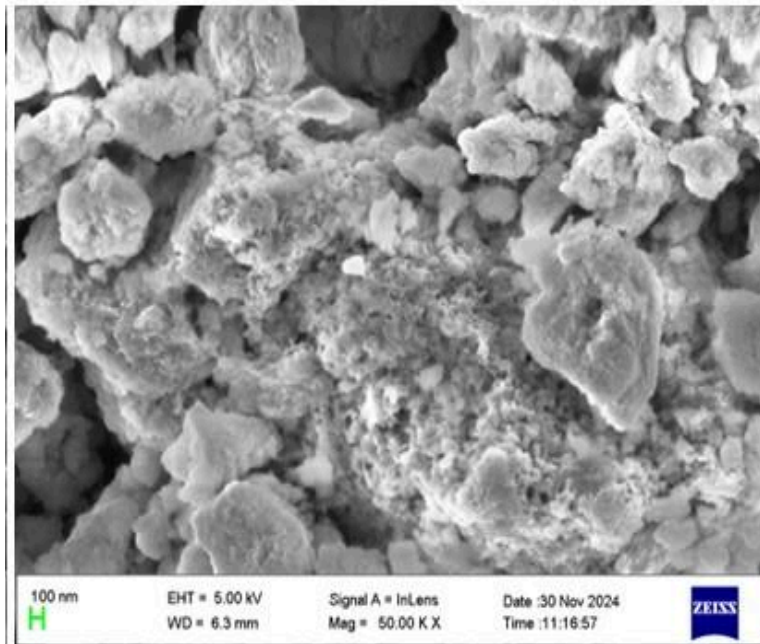


Fig 3.2: FESEM image of sample magnesium ferrite.

3.3 UV - VISIBLE SPECTROSCOPY:

In this work optical characterization is done using UV visible absorption and photoluminescence. The prepared samples are studied using UV-Visible and PL spectra. The UV-Visible absorption spectra of magnesium ferrite nanoparticles prepared by sol-gel method is shown below. The characteristic peaks appear in the wavelength range 200-800 nm and the peak position reflects the band gap of the nanoparticles.

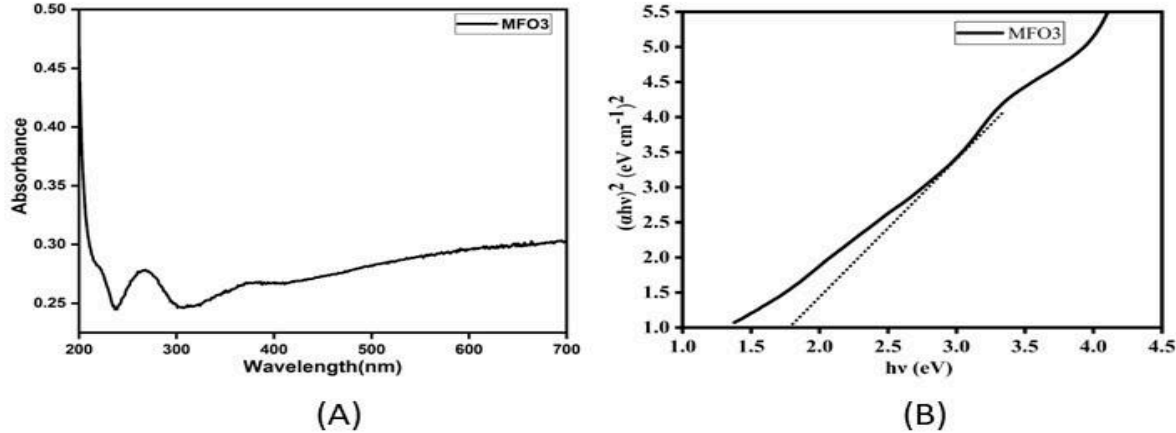


Fig 3.3 (A) Absorption spectrum of magnesium ferrite, (B) Tauc plot of magnesium ferrite

The UV-Visible absorption spectra of silver- doped magnesium ferrite nanoparticles prepared by sol-gel method is also shown below. The characteristic peaks appear in the wavelength range 200-800 nm and the peak position reflects the band gap of the nanoparticles. The fundamental absorption, which corresponds to electron excitation from the valence band to conduction band, can be used to determine the value of optical band gap of the synthesized magnesium ferrite nanoparticles.

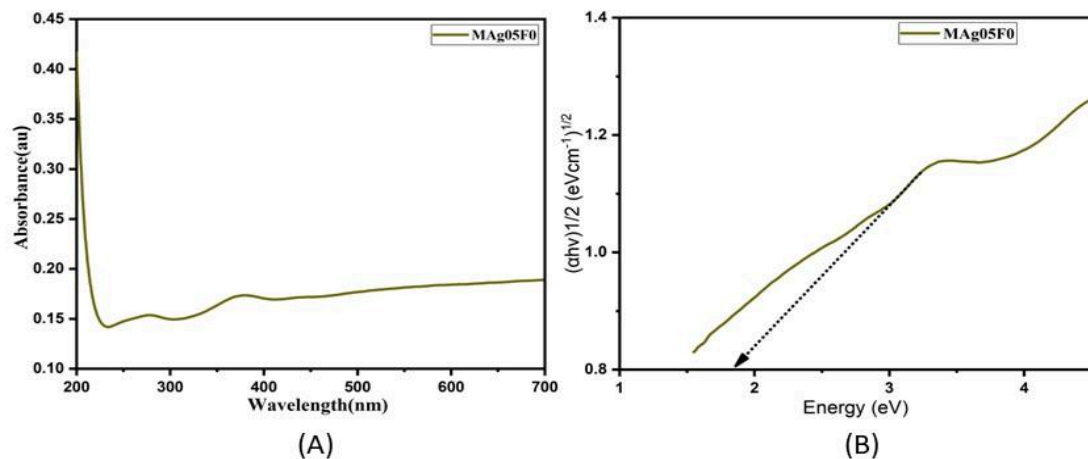


Fig 3.4 (A)-Absorption spectrum of silver- doped magnesium ferrite, (B)- Tauc plot of silver doped magnesium ferrite

Sample	Band gap (eV)
MFO 3	1.75
MAg05FO	1.86

Band gap energy can be calculated by the formula

$$E_g = \frac{hc}{\lambda}$$

Here h is the planck's constant, λ is the wavelength of absorption. From the optical absorption data, a graph is plotted with $h\nu$ versus $((\alpha h\nu)^2)$ to determine the band gap energy for the sample. By extrapolating the linear portion of the curve to meet $h\nu = 0$, one can calculate the band gap energy in eV. The figure shows the $h\nu$ versus $((\alpha h\nu)^{1/2})$ graph of magnesium ferrite nanoparticles prepared by sol gel method.

The band gap energy was calculated using Tauc's plot. According to Tauc's equation for a direct band gap material the absorption Coefficient near the band gap edges is :

$$\alpha = \frac{A}{h\nu} (h\nu - E_g)^{\frac{1}{2}}$$

Where Alpha is the absorption coefficient, $h\nu$ is the photon energy, E_g the band gap energy and A is a constant depending on the type of transition. About equation can be rearranged and written in the form:

$$(\alpha h\nu)^2 = A^2 (h\nu - E_g)$$

Band gap is an important parameter that determines the electrical conductivity of the materials. Band gap is the amount of energy required to promote a valence electron from Valence band to conduction band and the electron is free to move within the crystal lattice and serve as a charge carrier to conduct electric current. Hence the energy band gap of the ferrite nanoparticles are important for allowing devices to operate at higher temperatures under normal conditions. This property makes them highly attractive for applications.

The band gap of pure magnesium ferrite which was calcined at 800°C was found to be 1.75 eV. But when silver is added at a concentration of 0.05 there should be some random changes and the band gap changes to 1.86 eV, indicating modification of electronic structure, and this alteration enhances the material's photothermal conversion efficiency.

3.4 FOURIER TRANSFORM INFRARED SPECTROSCOPY

The FTIR spectra of pure magnesium ferrite show peaks at 1488.55 cm^{-1} , possibly related to carbonate groups or organic impurities, and 525.55 cm^{-1} , typically associated with metal-oxygen bonds (Fe-O or Mg-O) in the ferrite structure. Upon silver doping, the peaks shift to 1482.67 cm^{-1} and a new peak emerges at 1422.89 cm^{-1} . These changes suggest that silver doping influences the ferrite structure, leading to modifications in bond strengths and vibrational frequencies, and potentially alters the surface chemistry. The shifts in peaks indicate changes in carbonate groups or organic impurities, while the new peak may be related to interactions between silver and oxygen or other functional groups.

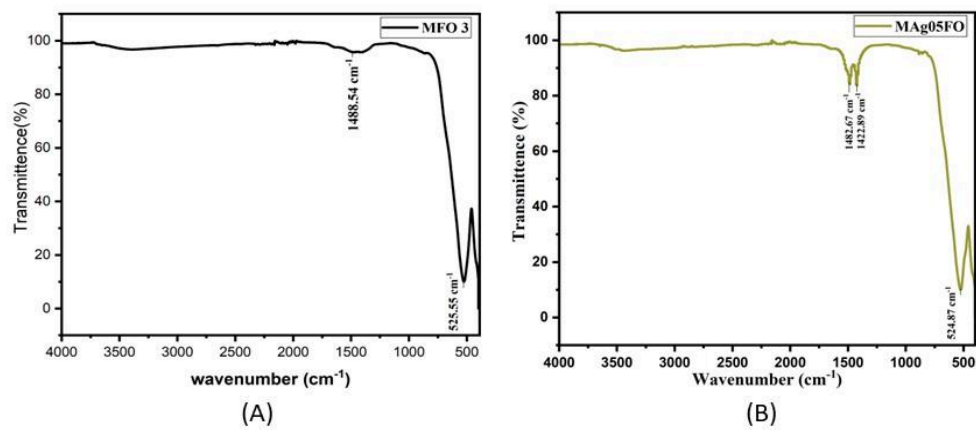


Fig 3.5 :(A) FTIR spectra for MgFe_2O (B) FTIR spectra for $\text{Ag}-\text{MgFe}_2\text{O}$

The FTIR analysis of pure magnesium ferrite and silver-doped magnesium ferrite reveals changes in the material's structural and chemical properties. Pure magnesium ferrite exhibits peaks at 1488.54 cm^{-1} and 525.55 cm^{-1} , indicating the presence of organic impurities and metal-oxygen bond vibrations. And silver doped at higher concentration of 0.05, the peaks at 1482.67 cm^{-1} and 1422.89 cm^{-1} suggest the presence of organic impurities or surface adsorbed species. The addition of silver to magnesium ferrite might enhance its photothermal activity, making it suitable for applications such as pollution remediation and energy-related devices. Further research could investigate the optimal silver concentration, mechanistic studies, and potential applications in various fields.

In conclusion, we understand that the addition of silver to magnesium ferrite alters its optical properties, as evident from changes in FTIR peaks indicating potential enhancements in photothermal activity. The shifts in emission wavelengths and presence of organic impurities suggest that silver incorporation modifies the material's electronic structure and surface properties.

3.5 PHOTOTHERMAL TECHNIQUES:

The thermal lens signal for both samples over a range of volume fractions was observed. The following graph shows the fitted curve (red) obtained for a particular volume fraction. The signal intensity is plotted along the Y-axis with time on the X-axis. The graph shows the variation of probe beam intensity with time.

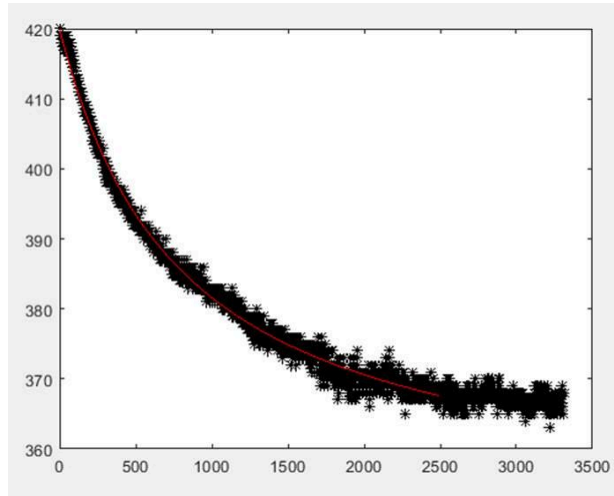


Fig 3.6 Thermal lens signal intensity graph

The value of t_c was obtained for each of the volume fractions and the values of thermal diffusivity were calculated using the equation

$$D_{\text{sample}} / D_{\text{water}} = t_{c \text{ water}} / t_{c \text{ sample}}$$

1. Magnesium Ferrite

Volume Fraction (μL)	Thermal Diffusivity D ($\times 10^{-7} \text{ m}^2/\text{s}$)
5	0.507384
20	0.094022
30	0.749261
40	0.373845
50	1.594622
60	0.740579
70	0.526145

2.Silver-doped Magnesium Ferrite

Volume Fraction (μL)	Thermal Diffusivity D ($\times 10^{-7} \text{ m}^2/\text{s}$)
5	0.382151
20	0.66685
30	0.596883
40	0.324027
50	1.565791
60	2.817173
70	1.049983

A thermal diffusivity v/s volume fraction graph was plotted for both samples using the values from the table above.

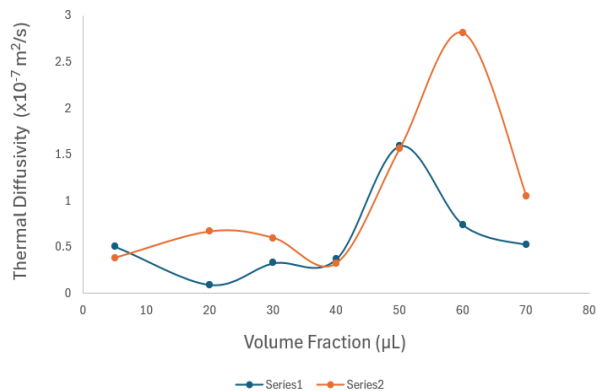


Fig 3.7 comparison graph of thermal diffusivity

The thermal diffusivity of undoped and silver-doped magnesium ferrite nanoparticles has been compared in the above graph. Series 1 (blue) shows undoped Magnesium Ferrite, and Series 2 (orange) shows Silver-doped Magnesium Ferrite

The thermal diffusivity of undoped Magnesium Ferrite peaks at $1.5946 \times 10^{-7} \text{ m}^2/\text{s}$ at a volume fraction of $50 \mu\text{L}$ before dropping off. This suggests that there is an optimal volume fraction for the highest thermal diffusivity. Meanwhile, Silver-doped Magnesium Ferrites peaks at $2.8171 \times 10^{-7} \text{ m}^2/\text{s}$ at a volume fraction of $60 \mu\text{L}$. It appears that silver doping causes the peak diffusivity of Magnesium Ferrite to become almost twice its undoped value.

3.6 ANTIBACTERIAL PROPERTY:

The antibacterial performance of various samples say magnesium ferrite and silver-doped magnesium ferrite or magnesium modified with silver was just examined against the *Staphylococcus aureus* (S. aureus) and *Escherichia coli* (E. coli) simply through the zone of inhibition (ZOI) testing. The cell-culture dish was immunized with the bacterial strain under aseptic conditions and wells were filled with the test samples and incubator at 37 degrees for 24 hours. After the incubation period the diameter of the growth inhibition zones were measured and recorded in centimetres. Pure magnesium ferrite didn't show any visible antibacterial activity against both strains, which is understood with the help of no inhibition zones surrounding the pure samples. This simply tells that , under some sufficient conditions, pure magnesium does not show sufficient bactericidal or simply the bacteriostatic effects on either Gram-positive (S.aureus) or Gram-negative (E.coli) organisms.

However,with the modification or addition of silver into magnesium ,marked a gradual increase in the antibacterial response. Clear zone of inhibition around the silver doped sample indicates the suppression of bacterial growth. Notably, the inhibition zone is simply larger in the case of *S.aureus* than for *E.coli*, which indicates a higher sensitivity of the Gram-positive bacteria to the material.Silver ions are well-famous for their wide-spectrum antimicrobial properties,often damaging cellular respiration, damaging DNA, and compromising membrane integrity.

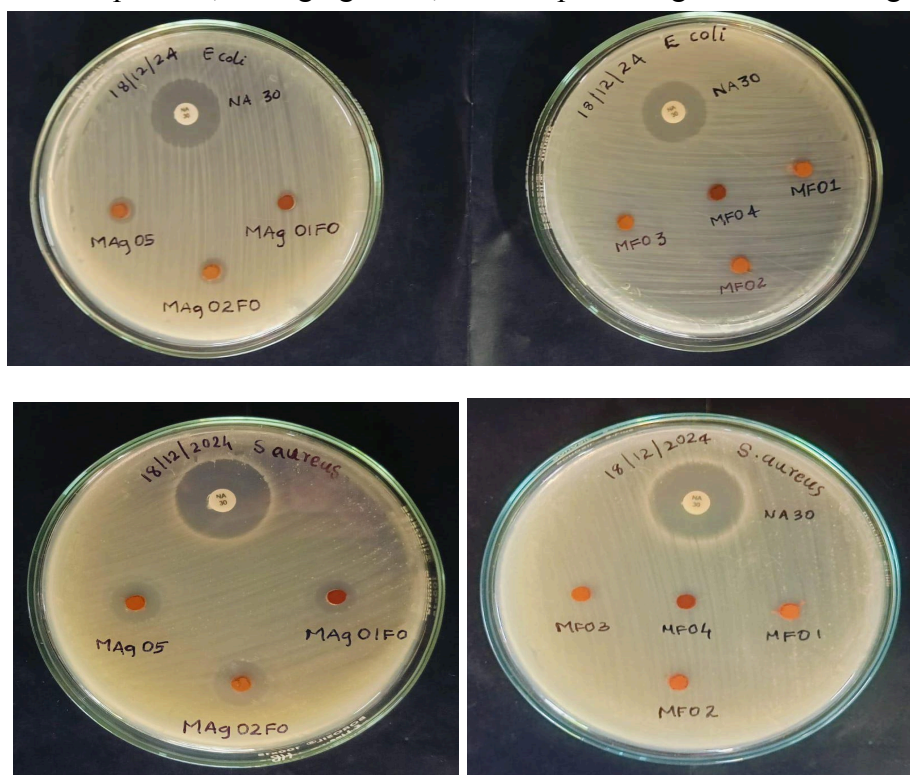


Fig 3.8 Antibacterial Studies

The increased sensitivity of *S. aureus* over *E. coli* observed can be attributed to the structural variations of the cell wall. The peptidoglycan layer in Gram-positive species such as *S. aureus* is thicker compared to Gram-negative species, and they do not have the outer membrane found in Gram-negative bacteria. This lack of an outer membrane is likely to enable silver ions to penetrate and interact with Gram-positive cells more readily, leading to larger inhibition zones.

In addition, battery-like galvanic effects at the metal interface could also play a secondary role in augmenting antibacterial activity. Upon silver and magnesium combination as a galvanic couple, localized electrochemical reactions could change the pH or produce reactive oxygen species (ROS), thus further inhibiting bacteria, particularly around the contact zone.

In general, the results indicate that pure magnesium is not inherently antibacterial under such test conditions but that modification with silver greatly enhances its performance, especially against Gram-positive bacteria such as *S. aureus*. This has implications for future applications of silver-modified magnesium in biomedical implants or devices where antimicrobial function is desired.

Name of the organism	Zone of inhibition (ZOI) (cm)	
<i>E- coli</i>	NA	2
	MAg05	1
	MAg01FO	0.6
	MAg02FO	1
	MFO3	0
	MFO4	0
	MFO1	0
	MFO3	0
<i>S.aureus</i>	NA	2.4
	MAg05	1.2
	MAg01FO	1
	MAg02FO	1.3
	MFO3	0
	MFO4	0
	MFO2	0
	MFO1	0

Table 3.9 Inhibition zones under *E-coli* and *S.aureus* of $MgFe_2O_4$ & $Ag-MgFe_2O_4$

CHAPTER: 4

4.1 CONCLUSION

This study focused on the synthesis, characterization, and evaluation of the photothermal and antibacterial properties of magnesium ferrite (MgFe_2O_4) and silver-doped magnesium ferrite ($\text{Ag}-\text{MgFe}_2\text{O}_4$) nanocomposites prepared via the sol-gel method. Magnesium ferrite, known for its magnetic and semiconducting behavior, demonstrated promising photothermal properties and moderate antibacterial activity. However, upon doping with silver, the nanocomposites exhibited notable improvements in crystallinity, particle size, optical absorption, and surface morphology, as evidenced by XRD, UV-Vis spectroscopy, FTIR and FESEM analysis. The photothermal studies using the thermal lens technique confirmed that silver doping enhanced the thermal diffusivity of the material, making it more effective for light-to-heat conversion—an essential characteristic for applications in photothermal therapy. And this study also demonstrates that silver doping significantly enhances the thermal diffusivity of magnesium ferrite (MgFe_2O_4) nanoparticles—achieving values nearly twice that of water. This remarkable improvement positions silver-doped ferrites as promising candidates for applications requiring efficient thermal management, especially in biomedical fields such as photothermal therapy and magnetic hyperthermia. Spinel ferrites are already known for their magnetic properties and excellent biocompatibility, making them suitable for targeted therapeutic approaches.

Given the rising interest in non-invasive cancer treatments, the ability of doped ferrite nanoparticles to rapidly and selectively elevate temperature holds immense clinical potential. The enhanced photothermal conversion observed in these materials could be particularly beneficial in hyperthermia-based tumor ablation, a technique that still grapples with the challenge of maintaining precise thermal control using safe, biocompatible agents.

Looking ahead, it is imperative to investigate how external stimuli—especially magnetic fields—modulate the thermal diffusivity of these doped ferrite systems. Such studies could uncover magneto-thermal coupling effects, further optimizing their performance in hyperthermic environments. Moreover, exploring a broader spectrum of dopants (such as rare earth elements or transition metals) could provide insights into tailoring the thermal, magnetic, and structural properties of ferrites to meet specific therapeutic or technological needs. By integrating ferrites with polymers, carbon-based materials, or bioactive agents, multifunctional platforms could be engineered for simultaneous diagnosis, therapy, and drug delivery.

Ultimately, the findings of this study open new avenues for the design of next-generation ferrite nanomaterials that merge high thermal diffusivity with magnetic tunability and biological safety—characteristics essential for advancing modern biomedical technologies.

Additionally, antibacterial analysis revealed that silver-doped MgFe_2O_4 showed superior inhibition against both *E. coli* and *S. aureus*, owing to the synergistic effect of silver ions and the magnetic ferrite matrix. Overall, the results confirm that while pure magnesium ferrite itself possesses desirable characteristics for biomedical and environmental applications, silver doping significantly amplifies these properties, establishing $\text{Ag}-\text{MgFe}_2\text{O}_4$ nanocomposites as potent multifunctional materials with enhanced photothermal efficiency and broad-spectrum antibacterial activity. This work not only reinforces the potential of ferrite-based nanomaterials in advanced applications but also opens new avenues for the design of doped nanostructures for targeted technological use.

4.2 FUTURE SCOPE

The current research aimed at the successful synthesis of magnesium ferrite (MgFe_2O_4) nanoparticles and silver-doped magnesium ferrite ($\text{Ag}-\text{MgFe}_2\text{O}_4$) nanoparticles via the sol-gel method, followed by a comprehensive analysis of their structural, optical, morphological, and antibacterial properties by means of techniques like X-ray diffraction (XRD), field emission scanning electron microscopy (FESEM), UV-Visible spectroscopy. Silver doping had a great impact on the crystallite size, optical band gap, and antibacterial efficacy, rendering the material better-suited for prospective biomedical and environmental uses. Photothermal properties were also explored, which underlined the fact that these nanoparticles can efficiently convert light to heat, and thus they show great promise to be used for photothermal cancer therapy. Additionally, antibacterial research indicated silver doping significantly amplified the bacterial inhibiting effect against frequent bacterial strains, which has new possibilities of developing antimicrobial coatings and health materials. In spite of the encouraging results achieved, there is enormous scope for future research in this field. Additional optimization of the concentration of silver doping can be investigated to adjust the magnetic, optical, and antibacterial properties for particular targeted applications. Functionalization of the surface of the nanoparticles synthesized with biocompatible agents can enhance their stability and targeting capability in biomedical applications. Additionally, detailed in vitro and in vivo biocompatibility tests are required to evaluate their safety profile before clinical applications. Expanding the investigation to the synthesis hybrid nanocomposites by including other dopants or polymers may provide multifunctional materials with improved magnetic, catalytic, and photothermal properties. For environmental science, the applications of these nanoparticles in water treatment, pollutant degradation, and heavy metal adsorption can be extensively explored on a larger scale to approach real-life environmental remediation strategies. In addition, the long-term stability, recyclability, and toxicological profile of such nanoparticles is important in terms of its effective use on the ground. The work directed toward enhancing the synthesis routes towards tighter control on particle size distribution, crystallinity, and surface chemistry at production levels will take these materials going from research into the industry into commercial practice. Lastly, ongoing studies towards enhancing photothermal conversion efficiency through varied light sources as well as using these materials to medical devices or photothermal therapy platforms might open doors to highly efficient, targeted, and minimally invasive therapeutic technologies.

REFERENCES

1. Abraham, Ann Rose, et al. "Defect-focused analysis of calcium-substitution-induced structural transformation of magnesium ferrite nanocrystals." *New Journal of Chemistry* 44.4 (2020): 1556-1570.
2. Abraham, Ann Rose, et al. "Magnetic performance and defect characterization studies of core–shell architectured MgFe₂O₄@BaTiO₃ multiferroic nanostructures." *Physical Chemistry Chemical Physics* 21.17 (2019): 8709-8720.
3. Abraham, Ann Rose, et al. "Defects characterisation and studies of structural properties of sol–gel synthesised MgFe₂O₄ nanocrystals through positron annihilation and supportive spectroscopic methods." *Philosophical Magazine* 100.1 (2020): 32-61.
4. Abraham, Ann Rose, and P. M. G. Nambissan. "Positron annihilation spectroscopy for defect characterization in nanomaterials." *Design, fabrication, and characterization of multifunctional nanomaterials*. Elsevier, 2022. 123-146.
5. Abraham, Ann Rose, et al. "Realization of enhanced magnetoelectric coupling and raman spectroscopic signatures in 0–0 type hybrid multiferroic core–shell geometric nanostructures." *The Journal of Physical Chemistry C* 121.8 (2017): 4352-4362.
6. Abraham, Ann Rose, Sabu Thomas, and Nandakumar Kalarikkal. "An Overview of Prospects of Spinel Ferrites and Their Varied Applications." *Theoretical Models and Experimental Approaches in Physical Chemistry* (2018): 117.
7. Poole, Charles P., and Frank J. Owens. *Introducción a la nanotecnología*. Reverté, 2007.
8. GEORGE, AKHILA. *PHOTOTHERMAL AND ANTIBACTERIAL STUDY OF Cu/Cu₂O/CuO NANOCOMPOSITE*. Diss. St. Teresas College, 2024.

9. Wahab, Mohammad Abdul. *Solid state physics: structure and properties of materials*. Alpha Science Int'l Ltd., 2005.
10. Raffi, Muhammad, et al. "Investigations into the antibacterial behavior of copper nanoparticles against *Escherichia coli*." *Annals of microbiology* 60 (2010): 75-80.
11. Perumbilavil, Sreekanth, et al. "Nonlinear transmittance and optical power limiting in magnesium ferrite nanoparticles: effects of laser pulsedwidth and particle size." *RSC advances* 6.108 (2016): 106754-106761.
12. Dash, Chandra Sekhar, et al. "Effective Removal of Tetracycline Hydrochloride Under Visible Light Using Cobalt Doped Magnesium Ferrite Nanoparticles."
13. Lagashetty, Arunkumar, Amruta Pattar, and Sangappa K. Ganiger. "Synthesis, characterization and antibacterial study of Ag doped magnesium ferrite nanocomposite." *Heliyon* 5.5 (2019).
14. Fantozzi, Erika, et al. "Silver doped magnesium ferrite nanoparticles: physico-chemical characterization and antibacterial activity." *Materials* 14.11 (2021): 2859.
15. Okasha, N. "Influence of silver doping on the physical properties of Mg ferrites." *Journal of materials science* 43 (2008): 4192-4197.
16. Senthamilselvan, T., et al. "Studies on silver-doped magnesium ferrite utilizing the sol-gel process in terms of structure, magnetism, electricity, and electrochemistry." *Journal of Molecular Structure* 1311 (2024): 138445.
17. Zim, Sk Hasnat Taref, et al. "Investigation of calcination temperature effect on crystallographic, morphological, optical, and magnetic properties of silver-doped magnesium ferrite nanoparticles." *Next Nanotechnology* 7 (2025): 100140.

